DOCTORAL THESIS

Molecular Physiological Studies on the Role of Purine Ring Catabolism in Stress Acclimation of Plants

Shunsuke Watanabe

Department of Mathematical and Life Sciences

Graduate School of Science

Hiroshima University

2013

DECLARATION OF CO-AUTHORSHIP/PREVIOUS PUBLICATION

I. Co-Authorship Declaration

I hereby declare that this thesis incorporates material from joint research. I certify that I have essentially done all the work and obtained written permission from each of the co-authors to include the above material in my thesis.

I certify that, with the above qualification, this thesis and the work to which it refers are the results of my own efforts.

II. Declaration of Previous Publication

This thesis includes one original paper that has been published in a peer-reviewed journal:

Authors: Watanabe, S., Matsumoto, M., Hakomori, Y., Takagi, H., Shimada, H. and Sakamoto, A.
Article title: The purine metabolite allantoin enhances biotic stress tolerance through synergistic activation of abscisic acid metabolism
Journal: *Plant, Cell & Environment* (in press)
Publisher: Jon Wiley & Sons Ltd
DOI: 10.1111/pce.12218
Article first published online: 8 November 2013
Accepted manuscript online: 15 October 2013

I certify that I have obtained a written permission from the copyright owner to use the above-published material in my thesis. It is noted that, where it was necessary, the original text is slightly modified to fit the formatting and structuring style of the thesis. I certify that the above material describes work completed during my registration as graduate student at Hiroshima University.

Contents

Abbreviations

AAH .....allantoate amidohydrolase
ABA .....abscisic acid
ALN .....allantoinase (allantoin amidohydrolase)
AMP .....adenosine monophosphate
AS .....allantoin synthase
ATP .....adenosine triphosphate
BGLU .....β-glucosidase
ER .....endoplasmic reticulum
GMP .....guanosine monophosphate
GS .....glutamine synthetase
LB .....left border
IMP .....inosine monophosphate
MS .....Murashige and Skoog
MW .....molecular weight
NCED.....9-*cis*-epoxycarotenoid dioxygenase
NiR .....nitrite reductase
NOS .....nopaline synthase
NPTII .....neomycin phosphotransferase II
PAGE .....polyacrylamide gel electrophoresis
PBS .....phosphate-buffered saline
PCR .....polymerase chain reaction
PEG .....polyethylene glycol
RB .....right border
Rbc .....ribulose-1,5-bisphosphate carboxylase/oxygenase
RNAi .....RNA interference
ROS .....reactive oxygen species
RT-PCR .....reverse transcription-PCR
SDS .....sodium dodecyl sulfate
T-DNA .....transferred DNA
TAIR .....The Arabidopsis Information Resource
TBS .....Tris-buffered saline
UAH .....ureidoglycolate amidohydrolase
UGAH .....ureidoglycine aminohydrolase
UOX .....urate oxidase
VHA-A .....subunit A of vacuolar ATP synthase
WT .....wild-type
XDH .....xanthine dehydrogenase
XMP .....xanthosine monophosphate

GENERAL INTRODUCTION

Purine bases are heterocyclic organic nitrogen compounds ubiquitously found in all organisms. They are not only crucial building blocks of nucleic acids, nucleotides and nucleosides, but also serve as intracellular energy-storage depots, metabolic regulators and metabolic reaction intermediates. These vital roles in various biochemical pathways of primary and secondary metabolisms are essential for a number of cellular processes. Owing to high nitrogen content, purine bases, both endogenously produced and exogenously taken up, are also used as invaluable nitrogen resource in certain organisms under particular conditions such as nutrient deficiency. In living organisms, purines and their derivatives are formed and disassembled consecutively, with cellular levels intensively regulated by the metabolic processes of *de novo* synthesis, salvage and degradation.

Purine metabolism

The *de novo* synthesis of purines comprises a total of ten enzymatic reactions that require, besides amounts of energy input (ATP), various precursor molecules including phosphoribosylpyrophosphate, amino acids, 10-formyl tetrahydrofolate and carbon dioxide (Zrenner *et al.* 2006). The first purine compound formed in the *de novo* pathway is IMP. Therefore, other purine nucleotides such as AMP and GMP originate from IMP, and these purine nucleotides are subsequently utilized as substrates for building up DNA and RNA or generating other metabolic compounds. Although free purines and purine nucleosides are continuously released through

cellular breakdown of nucleotides, nucleic acids and other purine-containing compounds such as *S*-adenosyl amino acids, these partially degraded purine compounds are salvaged for nucleotide regeneration (Wasternack 1982; Crozier *et al*. 2000). Salvaging purine bases and nucleosides has obvious advantage over the *de novo* synthesis of purine nucleotides because the salvage reactions cost much less in terms of energy and material consumption. Therefore, the salvage pathway shares an important role with the *de novo* synthesis in the cellular homeostasis of purine nucleotide levels.

In contrast to the *de novo* synthesis and salvage pathways, the catabolism of purines plays different roles in organisms, and therefore has not been conserved in eukaryotic evolution (Zrenner *et al.* 2006; Werner and Witte 2011; Fig. 1). In the degradation, all purine bases and related compounds are converged to free xanthine, the first common intermediate of the catabolic pathway. Although plants conserve the complete oxidation pathway of purine ring that ultimately liberates the ring nitrogen as ammonium (Moffatt and Ashihara 2002), animals decompose it only partially due to the successive loss of catabolic enzymes after terrestrialization (Hayashi *et al*. 2000). This evolutionary consequence eliminates the possibility of the toxic ammonia formation from purines, allowing most land animals to excrete either uriate or the ureide allantoin as unusable nitrogenous waste (Vogels and Drift 1976). For example, in primates, birds or reptiles, urate is the endproduct of purine degradation, whereas most mammals generate allantoin for excretion. By contrast, inorganic nitrogen including ammonia is an essential but environmentally scarce macronutrient required by plants for normal growth and reproduction. Therefore, it is generally accepted that the full breakdown of

purine bases benefits the needs of plants for nitrogen by re-assimilating the released ammonium into organic compounds (Zrenner *et al*. 2006).

The pathway of purine catabolism in plants

Plant purine catabolism has a relatively long history of physiological and biochemical studies, particularly in leguminous species, because it constitutes an integral part of the storage and xylem translocation of symbiotically fixed nitrogen (Schubert 1986; Smith and Atkins 2002). Only recently, however, have the pathway and the enzymes involved in each step of purine catabolism been identified at the molecular and biochemical levels, mainly using the model plant *Arabidopsis thaliana* (Werner and Witte 2011; Fig. 1). In plants, purine ring catabolism involves seven enzymes that are distributed in three subcellular compartments: cytosol, peroxisome, and endoplasmic reticulum (ER). The initial reaction is catalyzed by xanthine dehydrogenase (XDH) to oxidize xanthine, yielding urate in the cytosol (Datta *et al*. 1991; Hesberg *et al*. 2004). Urate is then transported into the peroxisomes where it is converted to allantoin *via* a three-step reaction, first mediated by urate oxidase (UOX) and then by allantoin synthase (AS), the bifunctional single enzyme previously known as a transthyretin-like protein (Lamberto *et al*. 2010; Pessoa *et al*. 2010). The subsequent pathway for ureide degradation, which takes place in the ER, is composed of four enzymes that hydrolyze allantoin sequentially to derive four molecules of ammonium. Allantoin and its hydrolytic product, allantoic acid, are degraded to ureidoglycine, by allantoinase (ALN, also known as allantoin amidohydrolase; Yang and Han 2004) and allantoate amidohydrolase (AAH; Todd and Polacco, 2006), respectively. This ureido

intermediate is finally degraded to ammonium and glyoxylate, the nitrogen-free product of the terminal reactions of this pathway, by the two most recently identified enzymes, ureidoglycine aminohydrolase (UGAH; Serventi *et al*. 2010) and ureidoglycolate amidohydrolase (UAH; Werner *et al*. 2010).

Possible role of purine catabolism in stress acclimation of plants

Although attributed to source-to-sink nitrogen remobilization, the role of purine degradation might not be restricted to housekeeping tasks, as several recent reports cite its close association with plant responses and adaptation to stress. It has been documented that various plants respond by gene induction and activation of the pathway enzymes to abiotic and biotic stress such as drought (Yesbergenova *et al*. 2005; Alamillo *et al*. 2010), high salinity (Sagi *et al*. 1998; Hesberg *et al*. 2004), and pathogen invasion (Montalbini 1995), or upon the stress hormone abscisic acid (ABA) treatment (Hesberg *et al*. 2004; Yesbergenova *et al*. 2005; Alamillo *et al*. 2010). Stress-induced alteration of purine catabolism is also evident at the metabolite level, as the ureides, notably allantoin, accumulate in response to stress conditions (Montalbini 1991; Sagi *et al*. 1998; Nikiforova *et al*. 2005; Brychkova *et al*. 2008; Alamillo *et al*. 2010; Kanani *et al*. 2010; Rose *et al*. 2012). When exogenously applied, allantoin alleviates oxidative damage symptoms from a tissue to a whole-plant level (Gus'kov EP *et al*. 2004; Brychkova *et al*. 2008; Wang *et al*. 2012). More recently, reverse genetic approaches have been adopted to examine the role of purine catabolism in plant physiological processes including growth, development and stress responses. For example, Arabidopsis mutants defective in XDH,

the critical bottleneck to purine oxidation and subsequent ureide hydrolysis (Fig. 1), display precocious senescence (Nakagawa *et al*. 2007a; Brychkova *et al*. 2008) and become hypersensitive to drought stress (Watanabe *et al*. 2010) and prolonged darkness (Brychkova *et al*. 2008). The increased stress sensitivity of XDH-impaired *Arabidopsis* may result from purine metabolite deficiency as the simultaneous treatments with exogenous urate or ureides rescued the *XDH*-knockout/knockdown phenotype (Nakagawa *et al*. 2007a; Brychkova *et al*. 2008; Watanabe *et al.* 2010). Although these reverse-genetic studies support the view that purine catabolism play a role in plant defense against environmental stress, it remains largely unknown how purine metabolites are involved in stress protection of plants.

The aim of this study

The primary motivation of this study was to elucidate a possible role of purine catabolism in plant stress protection and to identify purine metabolite(s) that play a crucial role in the mechanism of stress tolerance of plants. Among several purine intermediate metabolites formed during the catabolic process (Fig. 1), I focused particularly on allantoin because this ureide compound has been reported as a major purine metabolite in various plants under environmental adversities. To address the aims, I investigated thoroughly the possible protective effects of its accumulation on plant performance under stress conditions, using the model plant *Arabidopsis thaliana.* In CHAPTER I, I established Arabidopsis knockout mutants (*aln*) that impaired the allantoin-degradation step, leading to constitutively high levels of allantoin in the mutant plants. I examined the tolerance of these mutants to water-deficit stress such as drought shock and high osmosis, and

showed evidence that the accumulation of allantoin enhanced abiotic stress tolerance of Arabidopsis. In CHAPTER II, I attempted to elucidate how allantoin mediates the enhanced stress tolerance. For this purpose, I examined the molecular physiological aspects of the effect of allantoin accumulation, especially on global gene regulation by performing genome-wide gene expression analysis of an *aln* mutant. These analyses showed that allantoin accumulation resulted in dramatic alteration in the transcriptome profiles, accompanied with the significant up-regulation of stress/abscisic acid (ABA)-responsive genes. Finally, in CHAPTER III, I examined the mechanism by which allantoin elicits ABA-mediated stress responses, which revealed the unexpected connection of purine degradation to ABA production in the regulation of plant acclimatization to abiotic stress.

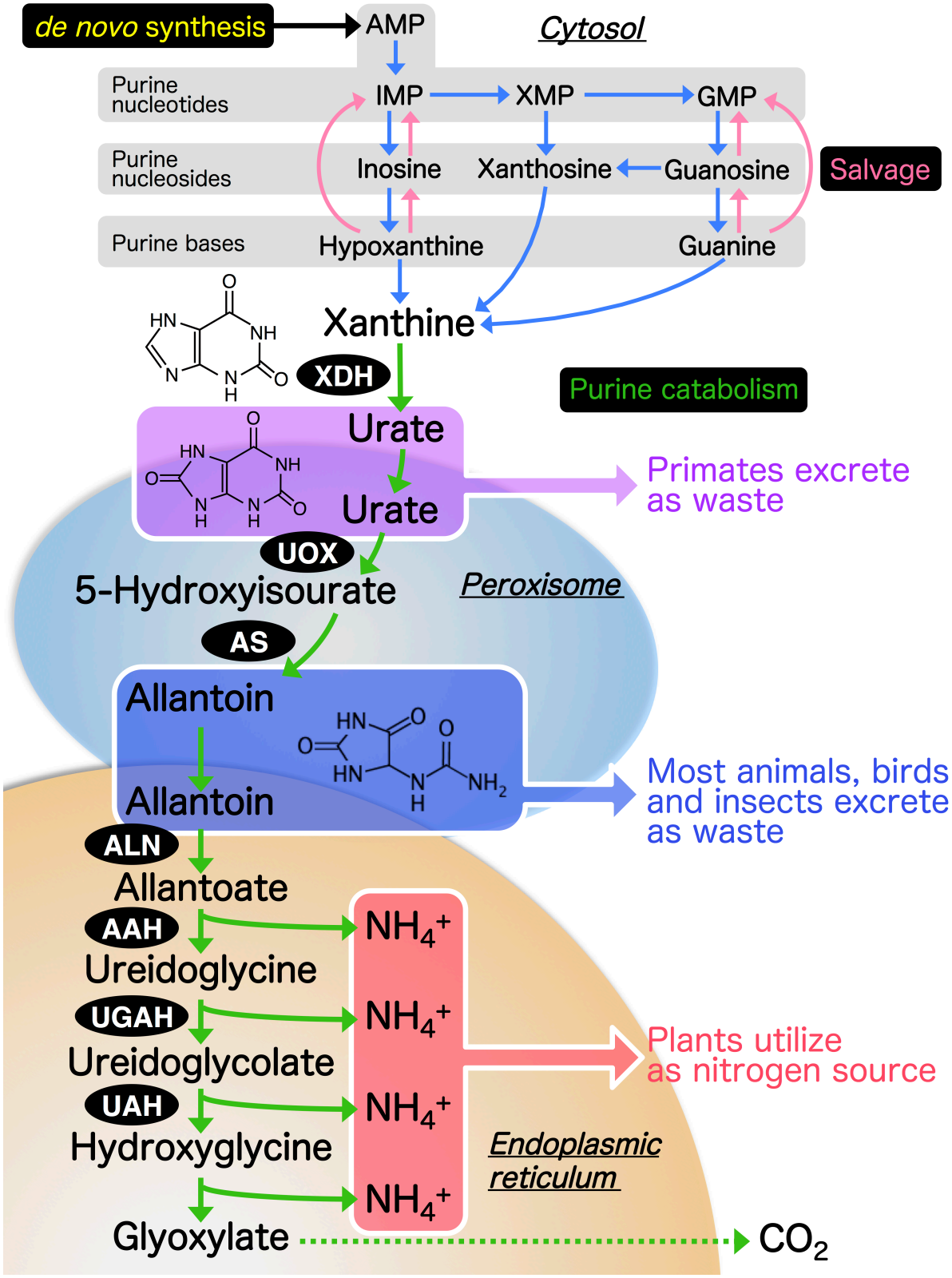

Figure 1. Overview of purine catabolism.

Pink and green arrows indicate the routes of salvage and catabolic pathway, respectively. Only enzymes involved in the catabolic pathway are shown: XDH, xanthine dehydrogenase; UOX, urate oxidase; AS, allantoin synthase; ALN, allantoinase (allantoin amidohydrolase); AAH, allantoate amidohydrolase; UGAH, ureidoglycine aminohydrolase; UAH, ureidoglycolate amidohydrolase. Note that, besides xanthine oxidation, XDH also catalyzes the conversion of hypoxanthine to xanthine.

CHAPTER I

Identification of Allantoin as a Purine Intermediary Metabolite Involved in Stress Tolerance of Arabidopsis

Introduction

For long, purine catabolism has been regarded as serving a cellular housekeeping function that remobilizes nitrogen for plant growth, development and reproduction. However, emerging evidence from physiological, biochemical and recent reverse-genetic studies suggests that certain purine metabolites might contribute to stress protection of plants. These studies report: (i) Purine-catabolic pathway is activated by biotic and abiotic stresses, which results in increased accumulation of mRNA and augmented activities of the catabolic enzymes (Montalbini 1995; Hesberg *et al*. 2004; Yesbergenova *et al.* 2005; Brychkova *et al*. 2008); (ii) Certain metabolic intermediates, notably allantoin and allantoate, accumulate as major purine catabolites in a variety of plants under stress conditions such as high salinity, drought and extended darkness, pathogen attack, or under nutrient deprivation (Sheoran *et al*. 1981; Montalbini 1991; Nikiforova *et al*. 2005; Brychkova *et al.* 2008; Alamillo *et al*. 2010; Kanani *et al*. 2010); (iii) The ureide allantoin is proposed to act as anti-oxidative agent (Gus'kov *et al*. 2004; Brychkova *et al*. 2008); and (iv) Disrupting purine catabolism by silencing or knocking-out XDH, the bottleneck enzyme of the catabolic pathway, causes a stress-hypersensitive phenotype of Arabidopsis (Brychkova *et al*. 2008; Watanabe *et al*. 2010). In the work by

Watanabe *et al*. (2010), I demonstrated that dysfunction of purine catabolism significantly reduced the drought tolerance of Arabidopsis in which *XDH* expression is post-transcriptionally silenced by RNA interference (RNAi). As the hypersensitivity to drought stress of *XDH*-RNAi plants were recovered by the supplementation of urate, the immediate downstream metabolite of xanthine, it is possible to assume that certain purine intermediary metabolites might play a role in the acclimation to drought stress. Among several purine metabolites downstream of xanthine, allantoin is the most probable candidate because of its closest association with stress, as noted above.

Therefore, in this chapter, I examined the consequences of constitutively elevated levels of allantoin caused by Arabidopsis knockout mutants of ALN, the only known allantoin-degrading enzyme in plants to date, together with the other two knockout mutants of XDH and AAH that are impaired upstream and downstream of allantoin degradation, respectively (see Fig. I-1). I reasoned that if allantoin is intrinsically important in protecting plants against stress, its constitutive accumulation might improve plant performance under stress, thereby providing clues to the *in planta* mechanism by which this purine metabolite acts in stress protection.

Materials and Methods

Plant materials and growth conditions

Arabidopsis [*A. thaliana* (L.) Heynh.] accession Columbia-0 (Col-0) was used as wild-type (WT) and all mutant lines used in this work were in the Col-0 background. The seeds of the following SALK T-DNA insertion lines were obtained from the Arabidopsis Biological Resource Center (Ohio State University): *aln* (SALK_000325; Yang and Han 2004; also called *aln-1* in this work) and *aln-2* (SALK_146783, this study) disrupted in *ALN* [Arabidopsis Genome Initiative gene index (AGI): At4g04955]; *xdh1* (SALK_148366, this study; with the identical insertion site to SALK_148368 described in Yesbergenova *et al*. 2005) disrupted in *XDH1* (At4g34890); and *aah* (SALK_112631; Todd and Polacco 2006) disrupted in *AAH* (At4g20070). To identify homozygous T-DNA insertion lines, PCR-based genotyping of each mutant was performed using a gene-specific primer flanking the insertion in combination with a left-border T-DNA-specific LBa1 primer (Table I-1).

Surface-sterilized seeds from WT and transgenic plants were sown on 0.3% (w/v) gellan gum plates of standard medium consisting of a half-strength Murashige-Skoog (1/2MS) basal salts and 1% (w/v) sucrose. After incubation at 4ºC for 2 days, the plates were placed in a growth cabinet maintained at 22ºC under white fluorescent light with a 16-h photoperiod (70 μmol photons m^{-2} s^{-1}). To test the effect of metabolite supplementation, surface-sterilized seeds were dispersed on 1/2MS plate that had been supplemented with 10 mM allantoin as a sole nitrogen source. In control experiments, 10 mM NH_4NO_3 was used instead.

Genetic complementation

The complete *ALN* coding sequence was generated by PCR from cDNA made from total RNA of WT seedlings (for primers, see Table I-1). After sequence verification, the *ALN* coding sequence was cloned into pGWB14 (Nakagawa *et al*. 2007b) under the control of the cauliflower mosaic virus (CaMV) 35S promoter. The resulting recombinant binary plasmid carried by *Agrobacterium tumefaciens* strain GV3101 was introduced into the homozygous *aln-1* mutant plants through the floral-dip method as previously described (Clough and Bent 1998).

RNA isolation and quantitative real-time reverse transcription-PCR (qRT-PCR)

Total RNA was prepared from aerial parts of aseptically grown 2-week-old plants using the NucleoSpin RNAII extraction kit (Macherey-Nagel GmbH and Co). First-strand cDNA was synthesized using 1 µg of total RNA as a template, an oligo(dT) 18-mer primer, and the ReverTra Ace qPCR RT kit (Toyobo). Levels of various mRNAs were quantified by qRT-PCR using the KAPA SYBR FAST qPCR Kit (Kapa Biosystems, Inc.) in a 7300 Real-Time PCR System (Applied Biosystems). All PCR amplifications contained 1× KAPA SYBR Green Master Mix, 0.2 µM each primer, and 10 ng cDNA (total RNA equivalent) in a total volume of 20 µl. Gene-specific PCR primers were designed using Primer3Plus (http://www.bioinformatics.nl/cgi-bin/primer3plus/primer3plus.cgi) and primer sequences are listed in Table I-1. Relative gene expression data

were analyzed using the comparative $2^{-\Delta\Delta Ct}$ method (Livak and Schmittgen 2001) after normalization with *ACT2* as the control transcript. For semi-quantitative RT-PCR, aliquots of cDNA prepared from total mRNA of aseptically grown, 2-week-old seedlings were used as template. As internal control, transcripts of *VHA-A* encoding the subunit A of vacuolar ATP synthase were co-amplified with a target gene. The primers used for monitoring the transcription level were described in Table I-1.

Sodium dodecyl sulfate-polyacrylamide gel electrophoresis (SDS-PAGE) and immunoblotting

Immunoblotting analysis was carried out according to Nakagawa *et al*. (2007a). Briefly, total protein samples (20 μg) were prepared from aerial part of 2-week-old seedlings of WT and *xdh1* plants, subjected to SDS-PAGE using 7.5% polyacrylamide gel under reducing conditions, and electroblotted onto the polyvinylidene difluoride (PVDF) membrane (Immobilon-P; Millipore) in the transfer buffer [25 mM Tris, 200 mM glycine and 20% (v/v) methanol] with semi-dry methods. The blotted PVDF membrane was subsequently incubated for blocking in 0.3% (w/v) skim milk in phosphate buffered saline containing 0.05% (w/v) Tween-20 (PBS-T). Then the immunological reaction was performed using anti-XDH antibody [1:500 dilution in Tris-buffered saline (TBS: 50 mM Tris-HCl, pH 7.8, 0.1 mM $MgCl_2$, 0.15 M NaCl) containing 0.05% (w/v) Tween-20 (TBS-T)] as primary antibody and anti-rabbit IgG antibody conjugated to horseradish peroxidase (1:2000 dilution) as secondary antibody. Antigen-antibody complexes were detected by the chemiluminescence method with a Western Lighting Plus-ECL kit (PerkinElmer).

Stress treatments and assays

Drought shock was imposed as described in Watanabe *et al*. (2010). Aseptically grown 2-week-old seedlings were carefully removed from gellan gum plates and exposed to the air on a dry filter paper for 60 min. Alternatively, moist filter papers were used instead as control treatments. Wilted plants were then transferred back to gellan gum plates and allowed to recover for 7 days under the growth condition as described above. Survival was evaluated by counting seedlings showing total chlorosis as dead. To test osmotic stress tolerance, plants were grown on gellan gum plates of standard medium supplemented with mannitol, or on agar plates [1.5% (w/v) agar] that were infused with polyethylene glycol (PEG 8000; Sigma-Aldrich) to give a water potential of approximately –0.5 MPa according to the published protocol (Verslues *et al*. 2006). Sterilized seeds were sown on these media, and after a 2-day cold treatment, seedlings were grown in a growth chamber as described above. Alternatively, normally grown 3-day-old sterile seedlings were transplanted onto mannitol medium. Dry or fresh weight was scored after 14 days of growth or transplanting. Relative growth is expressed as a percentage of a whole plant weight in the absence of stress.

Determination of allantoin, allantoate, and chlorophyll

Allantoin and allantoate were determined after chemical transformation to glyoxylate by heat-induced alkaline-acid hydrolysis and acid hydrolysis, respectively (Todd and Polacco 2006). Briefly, aerial parts

of 2-week-old Arabidopsis seedlings were homogenized in liquid nitrogen, suspended with 50 mM potassium phosphate (pH 7.0), and centrifuged at 18,000 × *g* for 20 min. Subsequently, the supernatant was collected to the fresh tubes. For alkaline-acid hydrolysis of allantoin, collected samples were mixed with deionized H_2O and 0.5 M NaOH, and heated at 100 ºC for 8 min. Obtained alkaline-hydrolysates were incubated on ice for 5 min, mixed with 0.65 M HCl, and heated at 100 ºC for 4 min. Then, acid-hydrolysate samples were incubated on ice for 5 min, and then mixed with 60 mM Na_2HPO_4-KH_2PO_4 buffer (pH 7.0) containing 0.3% (w/v) phenylhydrazine · HCl. For acid-hydrolysis of allantoate, collected samples were mixed with deionized H_2O and 0.15 M HCl, and heated at 100 ºC for 4 min. Acid-hydrolysates were incubated on ice for 5 min, and then mixed with 60 mM Na_2HPO_4-KH_2PO_4 buffer (pH 7.0) containing 0.3% (w/v) phenylhydrazine · HCl. The hydrolyzed mixture was left for 5 min at room temperature, and incubated on ice. The mixture was colorized in precooled, concentrated HCl containing 0.15 % (w/v) potassium ferricyanide, after which the absorbance was read at 535 nm wavelength.

Chlorophyll was quantified as described previously (Nakagawa *et al*. 2007a).

Statistical analysis

All results are presented as means and standard errors of means (SEM). The difference between two groups was evaluated using Student's or Welch's *t*-test, depending on whether the variances of the compared samples were regarded as equal or not. Comparisons among three or more groups were made using one-way ANOVA with Tukey's multiple

comparison test, following Bartlett's test for homogeneity of variance. Testing was performed using R statistical software (version 2.15.2, R Development Core Team).

Results

Gene knockout of the enzymes involved in purine catabolism results in differential allantoin accumulation

To investigate the possible effects of constitutive allantoin accumulation on stress tolerance in Arabidopsis, I obtained two loss-of-function alleles for *ALN* from the SALK Institute T-DNA insertion collection. One insertion line (SALK_000325) was previously described as *aln* (Yang and Han 2004), and the other (SALK_146783) was newly characterized in this study (Figs. I-1a and I-2). For clarity, here I refer to the previously identified allele as *aln-1* and the newly characterized allele as *aln-2*. The results from PCR genotyping, qRT-PCR, and growth assays supported that each allele causes a defect in allantoin catabolism (Fig. I-2). In order to distinguish the specific effects of allantoin accumulation from general inhibitory effects on the purine-catabolic pathway, in this study, I also examined two other catabolic mutants, *xdh1* and *aah* (Figs. I-3 and I-4), which are defective in catabolic steps upstream and downstream of allantoin degradation, respectively (Fig. I-1a). Compared to WT, the steady-state allantoin levels increased 6-fold in both *aln-1* and *aln-2* mutants; by contrast, *xdh1* mutants exhibited significantly lower allantoin levels and *aah* mutants exhibited allantoin levels comparable to WT (Fig. I-1b). Allantoate, the immediate downstream metabolite of allantoin, accumulated about 6-fold more in the *aah* mutant but decreased significantly in *xdh1* and *aln* mutants (Fig. I-1b). The differential pattern of ureide accumulation signifies the specific step at which the catabolic pathway was impaired in each mutant.

aln *mutation enhances drought tolerance*

We tested the tolerance of the *aln* mutants to water deficit conditions created by drought shock or high osmoticum. First, we exposed 2-week-old sterile WT and *aln* seedlings to 60 minutes of air-drying, as we have done previously (Watanabe *et al*. 2010). After the treatment, when the wilted plants were returned to standard medium and allowed to grow for 7 days, only 66% of WT plants recovered (Fig. I-5a, b). In contrast, more than 85% of both *aln-1* and *aln-2* plants survived to maturity possibly because, upon recovery from drought shock, these *aln* mutants had better growth and more chlorophyll than WT plants (Fig. I-5c, d). To ascertain whether a mutation in the *aln* gene was responsible for the observed phenotype, the *aln-1* mutant was transformed with a complementation construct (Fig. I-6). Restoring *ALN* expression by genetic complementation reversed the drought-tolerant phenotype of the *aln-1* mutant (Fig. I-5a, b) as well as the ureide levels (Fig. I-6). These results indicate that loss-of-function mutations in the *ALN* gene resulted in enhanced drought-shock tolerance in Arabidopsis.

aln *mutation enhances osmotic stress tolerance*

Next, I tested whether the *aln* mutants enhance the ability to tolerate osmotic stress. In the presence of high osmolarity imposed by mannitol (100, 150, and 200 mM), the rates of seed germination were not significantly different between WT and the two *aln* mutants (Fig. I-7). However, after growth for 14 days on mannitol media, the *aln* mutants

grew better than WT (Fig. I-8a, b), suggesting that they are more tolerant to osmotic stress during seedling development. Corroborating results were obtained when post-germinated seedlings were subjected to 200 mM mannitol and the growth was compared between WT and *aln* mutants (Fig. I-8c, d). To further test the generality of osmotic stress responses, I exposed the *aln*, *xdh1* and *aah* mutants to another osmotic stress agent, PEG. As in the case of mannitol, the susceptibility at germination stage did not differ significantly among these genotypes (Fig. I-9). However, when grown for 27 days in medium with low water potential imposed by PEG, the two *aln* mutants had significantly more fresh weight as compared with WT or the other purine-catabolic mutants (Fig. I-10), indicating that the observed effect was specific to the *aln* mutation. Thus, I conclude that the *aln* mutation confers tolerance to general osmotic stress in Arabidopsis.

Elevated allantoin levels correlate with enhanced stress tolerance

To correlate purine metabolite levels with the observed stress tolerance, I measured changes in allantoin concentrations in WT and *aln* plants after stress treatments. Allantoin was consistently maintained at significantly higher levels in the two *aln* mutants than in WT, although allantoin levels increased in WT in response to drought or osmotic stress (Figs. I-5e and 8e). The results showed that *aln* mutations induced elevated allantoin accumulation that occurred consistently with increased stress tolerance.

Discussion

Two independent allelic mutations in *ALN* (*aln-1* and *aln-2*; Fig. I-2) resulted in higher accumulation of endogenous allantoin and enhanced the seedling growth and survival under drought and osmotic stress conditions (Figs. I-5, I-8 and I-10). Although the *aln-1* mutation was previously reported to have no effect on normal growth and development of Arabidopsis (Yang and Han 2004), the possible influence on stress responses and tolerance had remained unaddressed. Therefore, this study provided the first direct evidence for the role of allantoin in plant stress tolerance, supporting the importance of purine catabolism in stress protection of plants.

Allantoin accumulation as a result of *aln* mutation could bring about two possible effects on plant physiology: allantoin-specific effect and non-specific effect due to arrested purine catabolism. Therefore, there was a concern that the stress-tolerant phenotype of the *aln* mutants could result from the inhibition of normal purine catabolism. If this were indeed the case, the effect would not specific to allantoin but rather a non-specific side effect of the *aln* mutation. To address this critical point, I examined the effects of two more knockout mutations that affect different steps in the purine-catabolic pathway. Specifically, I used *xdh1* and *aah* mutants, which are impaired upstream and downstream of allantoin degradation, respectively (Figs. I-3 and I-4). Both *xdh1* and *aah* mutants accumulated much less allantoin than did the *aln* mutants, although purine metabolism was apparently disrupted by each mutation (Fig. I-1b). I evaluated osmotic stress tolerance of these mutants and confirmed that *xdh1* and *aah* mutations did not enhance stress tolerance (Fig. I-10). These results clearly

show that the effect of *aln* mutation is distinct from the possible side effect of arresting purine catabolism. Thus, the stress-tolerant *aln* mutant phenotype is in fact caused by the specific effect of *aln* mutation, hence by increased allantoin levels. These findings strongly suggest that allantoin has a key role in the observed stress-tolerant *aln* phenotype.

Table I-1. Nucleotide sequences of primers used in this study

AGI[a]	Gene symbol[b]	Direction	Sequence	Use
At4g04955	*ALN*	Forward	5’-CCTTTATGTGCCCTTCAGGA-3’ (F1)	PCR genotyping
		Reverse	5’-GGCCTATCACTCCACCAAGA-3’ (R1)	PCR genotyping
		Forward	5’-GGTAACTTCTTGGTGGAGTGATAGGC-3’	qRT-PCR and semi-qRT-PCR
		Reverse	5’-GGTTCCCACACAACAAGATCTGC-3’	qRT-PCR
		Forward	5’-CACCATGGAGAGAACTTTGCTTC-3’	Complementation
		Reverse	5’-TTAAGTAGTTGCAAGTTGCAG-3’	Complementation and semi-qRT-PCR
		Reverse	5’-GAGACCAAGAACTCCAGCATCTA-3’ (R3)	PCR genotyping
At4g34890	*XDH1*	Forward	5’-TGATGTTGGACAAATAGAAGGAGCGTTT-3’	qRT-PCR
		Reverse	5’-TATTCGGATTCCCCTTGAGAAGCGAAACA-3’	qRT-PCR
At4g20070	*AAH*	Forward	5’-CGGAGCTGATTGTACTATTGGAA-3’ (F2)	PCR genotyping
		Reverse	5’-GTCTTGAACCTCTCCTGTCATCTT-3’ (R2)	PCR genotyping
		Forward	5’-AACAACATTCCCACCTTGGTTAAGTGT-3’	qRT-PCR
		Reverse	5’-CACCCATAAGGATCTTCCTGTCTT-3’	qRT-PCR
At1g43160	*RAP2.6*	Forward	5’-GCTGTGACTAAAGAATGTGAAAGC-3’	qRT-PCR
		Reverse	5’-CCTTGTGTGGGTCTCGAATCTC-3’	qRT-PCR
At1g17180	*GSTU25*	Forward	5’-GTTTGGAATGAGGACGAGGA-3’	qRT-PCR
		Reverse	5’-AGGAGAATCGGGCTTTTGTT-3’	qRT-PCR
At5g37990	–	Forward	5’-ACAAGAAATCTCCGGCATTG-3’	qRT-PCR
		Reverse	5’-AGCTCTTGCCCCAAGAAAAT-3’	qRT-PCR
At3g28290	*AT14a*	Forward	5’-ATGGAGCAAATGAGGTGGAC-3’	qRT-PCR
		Reverse	5’-TTGCCACATCATCACCAACT-3’	qRT-PCR
At5g63450	*CYP94B1*	Forward	5’-TCCGACATCGTACCAACTCA-3’	qRT-PCR
		Reverse	5’-GAGATCGACGGTGATGGTTT-3’	qRT-PCR
At5g52310	*RD29A*	Forward	5’-AGGAACCACCACTCAACACA-3’	qRT-PCR
		Reverse	5’-ATCTTGCTCATGCTCATTGC-3’	qRT-PCR
At5g52300	*RD29B*	Forward	5’-ACGAGCAAGACCCAGAAGTT-3’	qRT-PCR
		Reverse	5’-AGGAACAATCTCCTCCGATG-3’	qRT-PCR
At4g27410	*RD26*	Forward	5’-AGTTCGATCCTTGGGATTTG-3’	qRT-PCR
		Reverse	5’-ACCCGTTGCTTTCCAATAAC-3’	qRT-PCR
At2g42540	*COR15A*	Forward	5’-GTCGATAACGAAGCCTTTGC-3’	qRT-PCR
		Reverse	5’-ATGCGGAAGACACAATCCTC-3’	qRT-PCR
At3g14440	*NCED3*	Forward	5’-CACTGGTAAATCTCGCTCTC-3’	qRT-PCR
		Reverse	5’-GTTACGTTGGAACTAGAAGC-3’	qRT-PCR
		Forward	5’-CACCTCTATAGATCTCGTCAAC-3’	*Fluc* fusion
		Reverse	5’-CATTTTTCAAGTGTGTTCAATCAGTAT-3’	*Fluc* fusion
At4g19230	*CYP707A1*	Forward	5’-TTGGAAAGAGGAGACTAGAG-3’	qRT-PCR
		Reverse	5’-CACTTGGTGTTTTCTCCTTG-3’	qRT-PCR
At2g29090	*CYP707A2*	Forward	5’-AAATGGAGTGCACTCATGTC-3’	qRT-PCR
		Reverse	5’-CCTTCTTCATCTCCAATCAC-3’	qRT-PCR
At5g45340	*CYP707A3*	Forward	5’-TCTTGTCCAGGCAATGAG-3’	qRT-PCR
		Reverse	5’-ATAGGCAATCCATTCTGAGG-3’	qRT-PCR
At3g19270	*CYP707A4*	Forward	5’-GAAAGGAATACAGTACAGTC-3’	qRT-PCR
		Reverse	5’-GGATTAGATTTGGCTAACTAC-3’	qRT-PCR
At3g18780	*ACT2*	Forward	5’-ACCGTATGAGCAAAGAAATCAC-3’	qRT-PCR
		Reverse	5’-GAGGGAAGCAAGAATGGAAC-3’	qRT-PCR
At1g78900	*VHA-A*	Forward	5’-ATGCCGGCGTTTTACGGAGG-3’	Semi-qRT-PCR
		Reverse	5’-ATTTCCCAATATTCCTGGCC-3’	Semi-qRT-PCR
	CaMV35S	Forward	5’-CTACAAATGCCATCATTGCG-3’ (CaMV)	PCR genotyping
–	T-DAN	–	5’-TGGTTCACGTAGTGGGCCATCG-3’ (LBa1)	PCR genotyping

[a]Arabidopsis Genome Initiative gene index (http://www.arabidopsis.org/portals/nomenclature/guidelines.jsp).

[b]Gene symbol as provided by TAIR (http://www.arabidopsis.org/) except LBa1 and CaMV35Spro, which refers to a primer specific to the left border of T-DNA of *Agrobacterium tumefaciens* and the 35S promoter region of *Cauliflower mosaic virus*, respectively

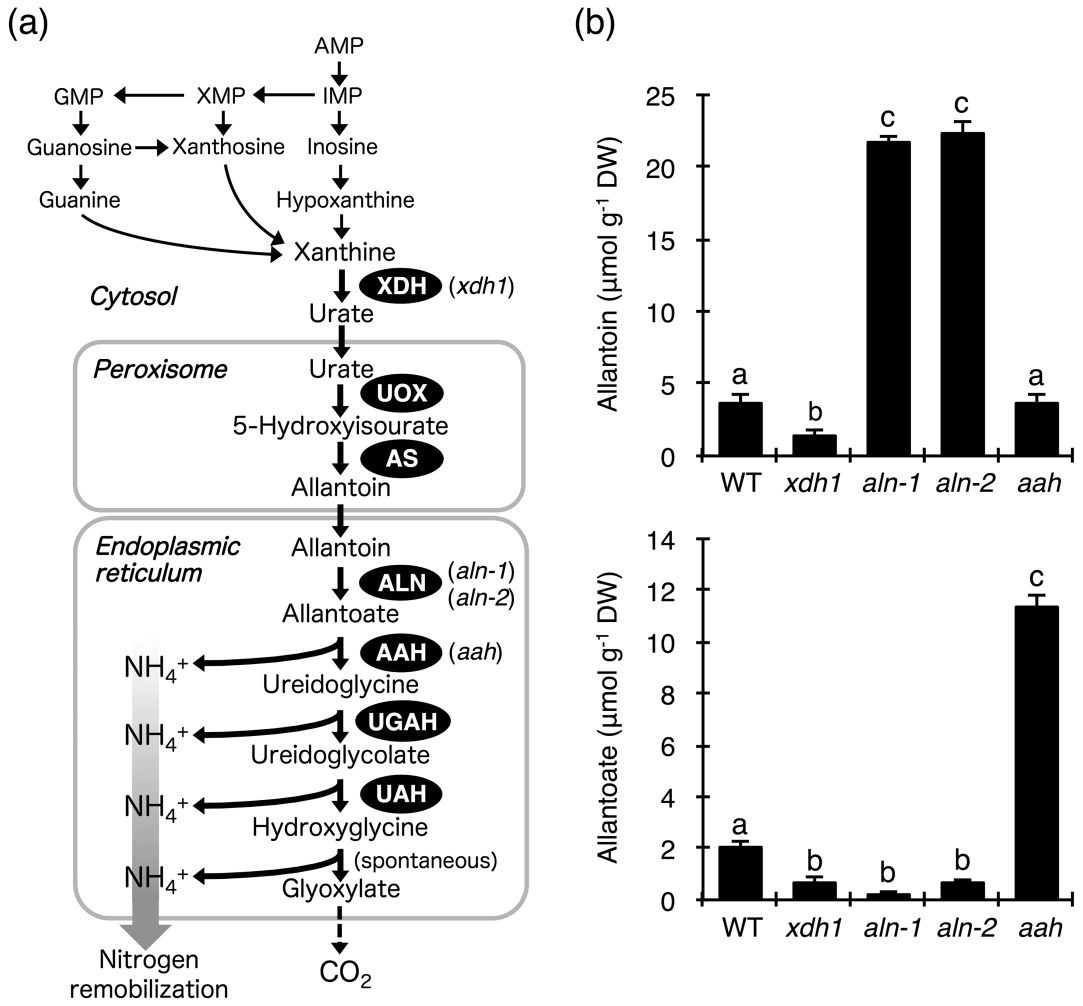

Figure I-1. Plant purine catabolism and knockout mutants used in this study.
(a) The catabolic pathway. Only enzymes involved in the main catabolic pathway starting from xanthine are shown and knockout mutants used in this study are indicated in parentheses after abbreviated enzyme names. XDH, xanthine dehydrogenase; UOX, urate oxidase; AS, allantoin synthase; ALN, allantoinase (allantoin amidohydrolase); AAH, allantoate amidohydrolase; UGAH, ureidoglycine amidohydrolase; UAH, ureidoglycolate amidohydrolase. Note that, besides xanthine oxidation, XDH also catalyzes the conversion of hypoxanthine to xanthine. (b) Levels of two major ureides, allantoin and allantoate, in aseptically grown 2-week-old seedlings of four knockout mutants of purine degradation used in this study (Figs. I-2 to I-4). DW, dry weight. Results are the mean of five independent experiments ± SEM. Different letters indicate significant difference among genotypes by one-way ANOVA with Tukey's multiple comparison test ($P < 0.05$).

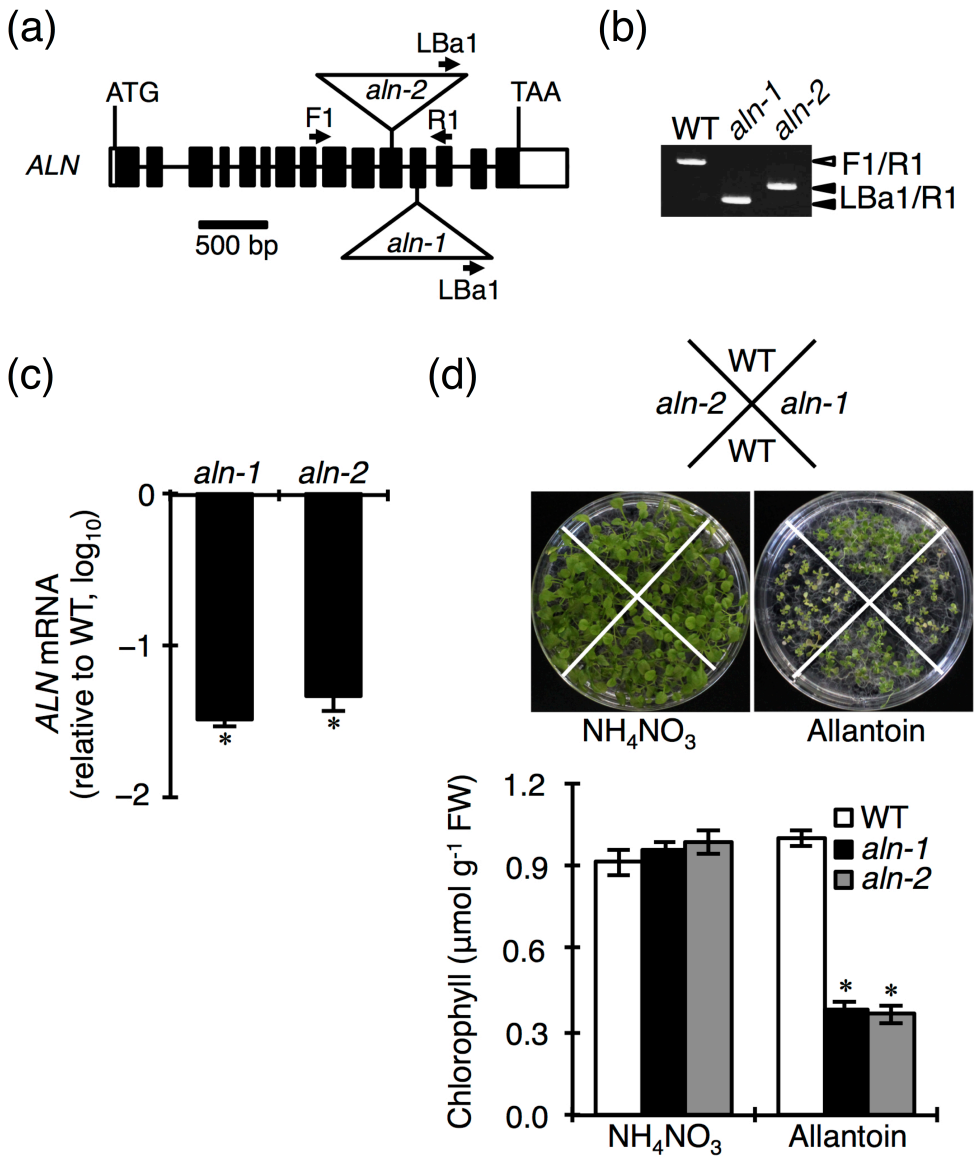

Figure I-2. Characterization of two allelic *aln* mutants.

(a) Diagram of T-DNA insertion in the *ALN* gene structure for two *aln* mutant alleles (*aln-1*, SALK_000325; *aln-2*, SALK_146783). Arrows indicate primers used for PCR-based genotyping. (b) PCR-based genotyping using *ALN* gene-specific F1 and R1 primers and a T-DNA-specific LBa1 primer. (c) qRT-PCR for estimating *ALN* mRNA levels in *aln-1* and *aln-2* mutants relative to WT expression after normalization to *ACT2* transcripts. (d) Apparent defects in ureide catabolism of the *aln* mutants as demonstrated by chlorotic growth on medium containing 10 mM allantoin as the sole nitrogen source. *Upper*: Plants after growth for 27 days. NH_4NO_3 (10 mM) was used in control growth. *Lower*: Chlorophyll content. FW, fresh weight. The results are the mean of three independent experiments ± SEM (*$P < 0.001$).

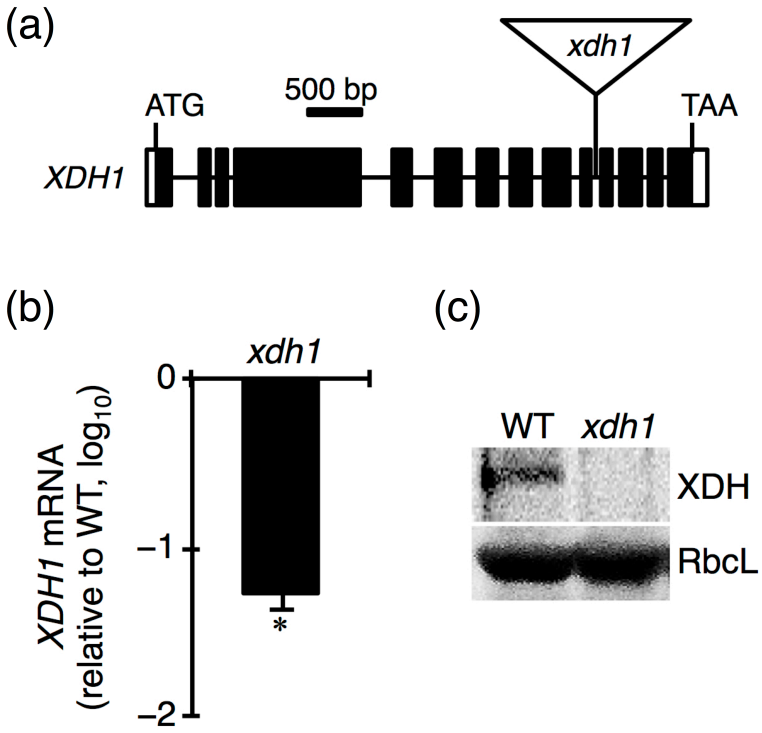

Figure I-3. Characterization of an *xdh1* mutant.

(a) Diagram of T-DNA insertion in the *XDH1* gene structure for an *xdh1* mutant (SALK_148366). (b) qRT-PCR for estimating *XDH1* mRNA levels in the *xdh1* mutant relative to WT expression after normalization to *ACT2* transcripts. (c) Immunoblotting analysis for XDH protein in the *xdh1* mutant. Twelve μg of total protein from rosette leaves of aseptically grown, 2-week-old WT and *xdh1* seedlings were resolved by SDS-PAGE (10 % polyacrylamide gel) and immunoblotted with anti-XDH antibody as described in Nakagawa *et al*. (2007a). Coomassie-stained RbcL provides a control for equal loading. The results are the mean of three independent experiments ± SEM (**P* < 0.001).

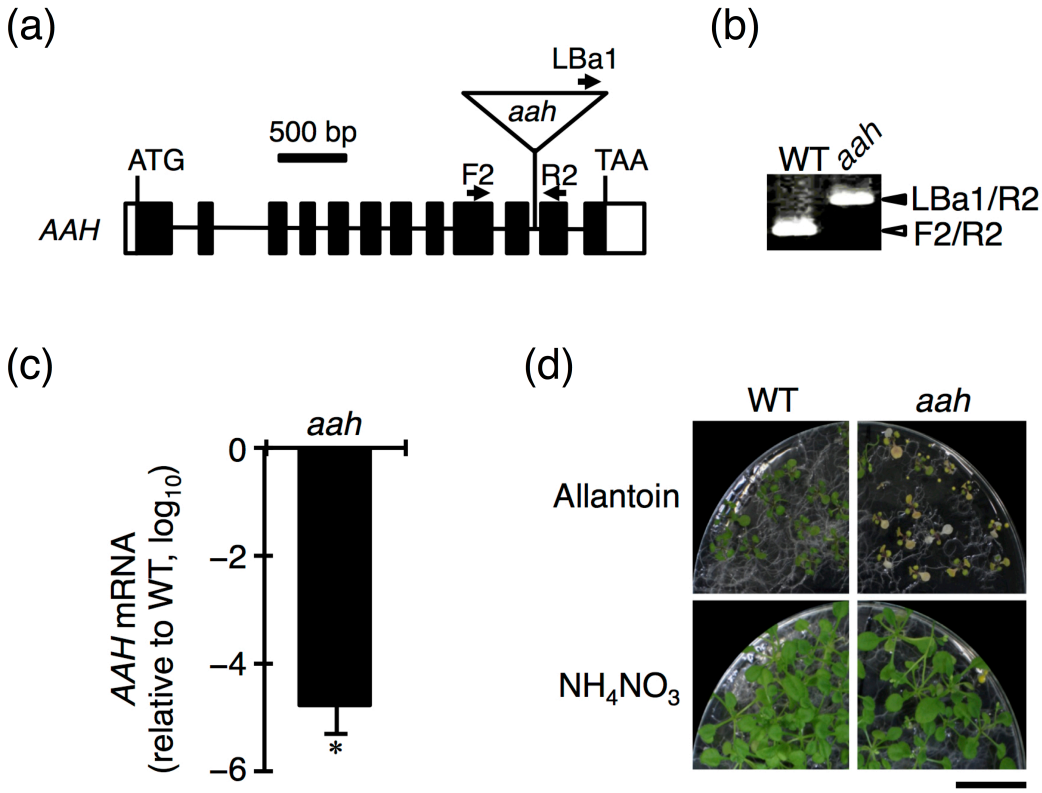

Figure I-4. Characterization of an *aah* mutant.

(a) Diagram of T-DNA insertion in the *AAH* gene structure for an *aah* mutant (SALK_112631). Arrows indicate primers used for PCR-based genotyping. (b) PCR-based genotyping using *AAH* gene-specific F2 and R2 primers and a T-DNA-specific LBa1 primer. (c) qRT-PCR for estimating *AAH* mRNA levels in the *aah* mutant relative to WT expression after normalization to *ACT2* transcripts. (d) Apparent defects in ureide catabolism of the *aah* mutant as demonstrated by chlorotic growth on medium containing 10 mM allantoin as the sole nitrogen source. Shown are plants after growth for 27 days (bar = 2 cm). NH_4NO_3 (10 mM) was used in control growth. The results are the mean of three independent experiments ± SEM (*P < 0.001).

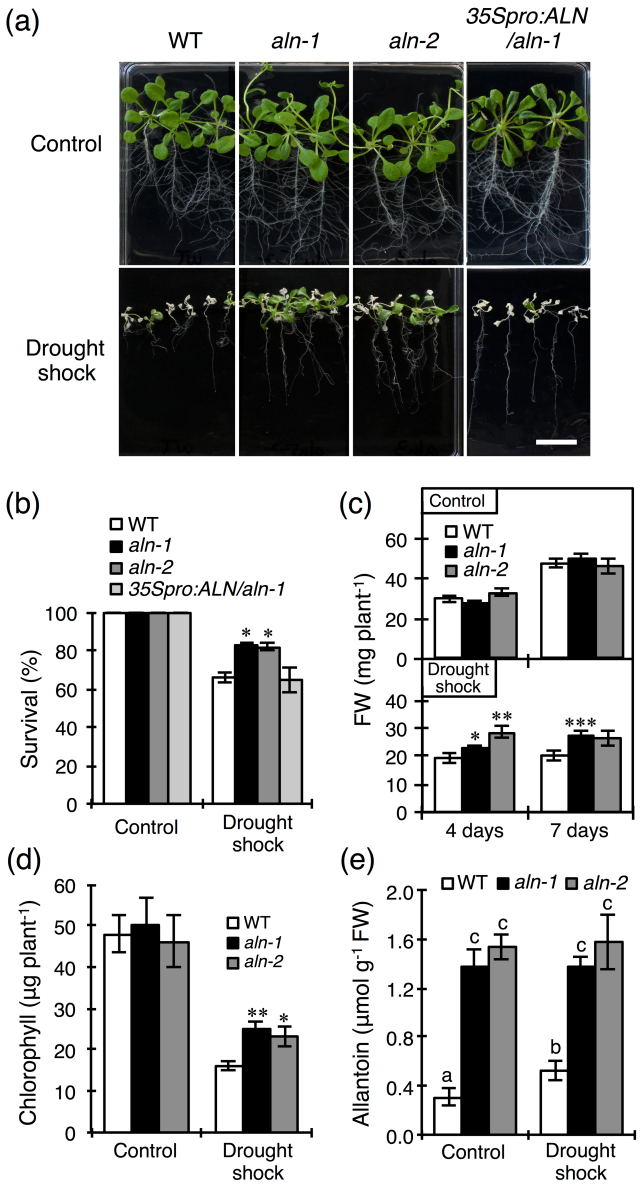

Figure I-5. Tolerance of *aln-1* and *aln-2* mutants to drought shock.

Aseptically grown 2-week-old seedlings from WT, two *aln* mutants and *ALN*/*aln-1* complementation line (*35Spro:ALN*/*aln1*; Figure I-6) were subjected to a 60-min drought shock, after which they were transferred back to the culture medium and grown for 7 days under standard conditions (a). Bar = 2 cm. Survival rate (b), biomass (c), chlorophyll content (d), and allantoin level (e) were evaluated for the seedlings 7 days after recovery from drought shock. FW, fresh weight. Results are the mean of three independent experiments ± SEM (*$P < 0.05$, **$P < 0.01$, ***$P < 0.001$). Different letters in (e) indicate significant difference by one-way ANOVA with Tukey-Kramer's test ($P < 0.05$).

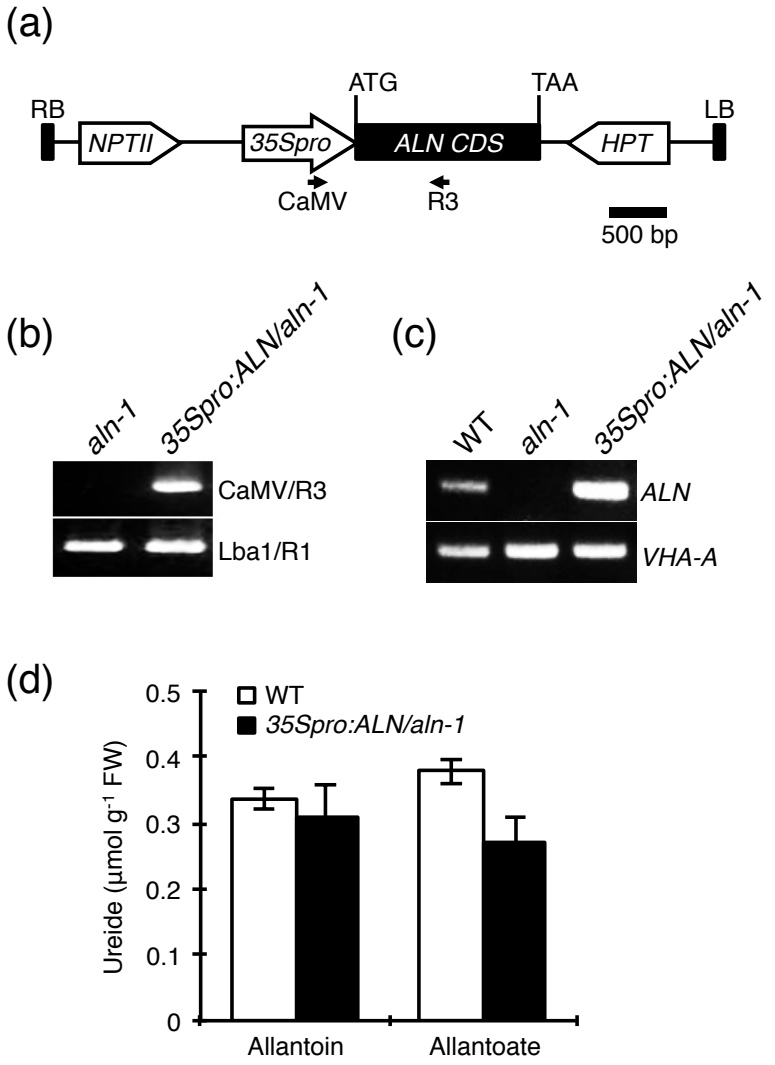

Figure I-6. Genetic complementation of *aln-1*mutation by *ALN* overexpression.
(a) Diagram of the overexpression cassette of *ALN*-coding sequence (CDS) under transcriptional control of the CaMV 35S promoter (*35Spro*). *NPTII* and *HPT* refer to genes conferring resistance to kanamycin and hygromycin, respectively. LB and RB denote left and right borders of the Ti binary vector pGWB14, respectively. Arrows indicate primers used for PCR-based genotyping. (b) PCR-based genotyping of a complementation line (*35Spro:ALN/aln-1*) using CaMV and R3 primers. LBa1 and R1 primers are the same as used in Figure I-2 to detect the *aln-1* mutant allele. (c) Semi-quantitative RT-PCR for estimating *ALN* mRNA levels in the complemention line. *VHA-A* expression was simultaneously analyzed as internal control (Nakagawa *et al*. 2007a). (d) Ureide (allantoin and allantoate) contents in 2-week-old sterile seedlings. FW, fresh weight. Results are the mean of three independent experiments ± SEM.

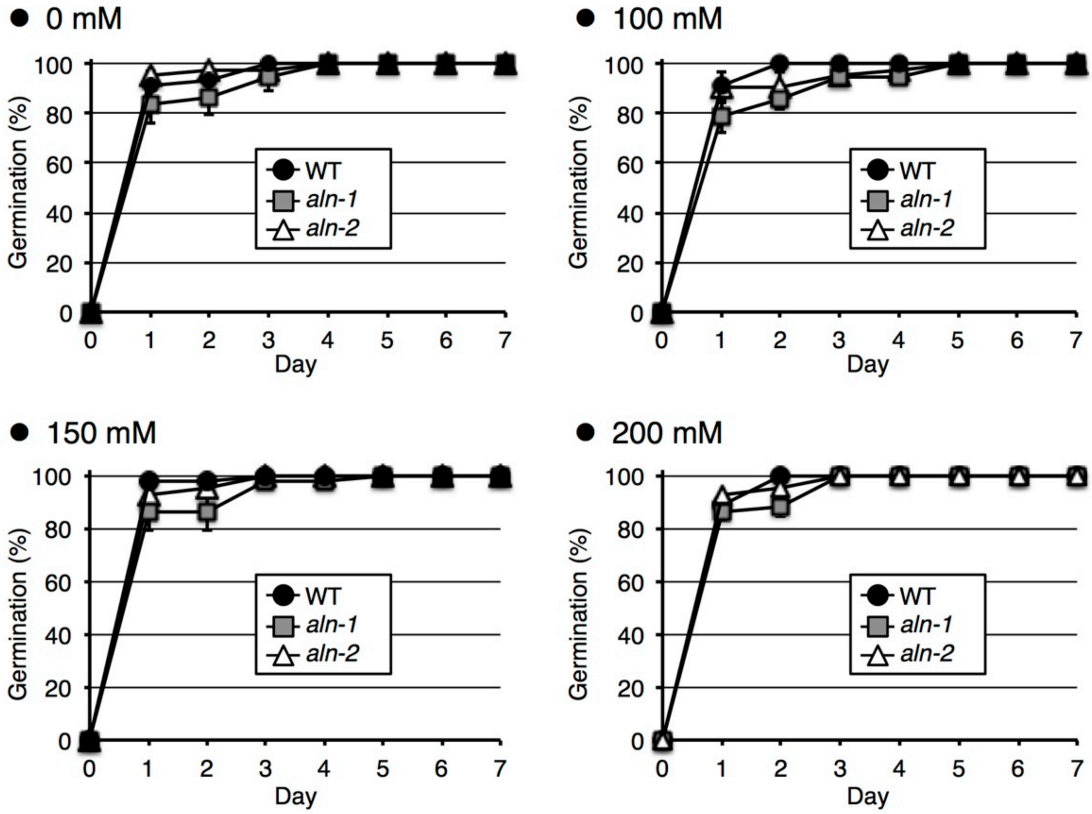

Figure I-7. Effects of osmotic stress imposed by mannitol on seed germination of WT and *aln* mutants.

Results are the mean of three independent experiments ± SEM.

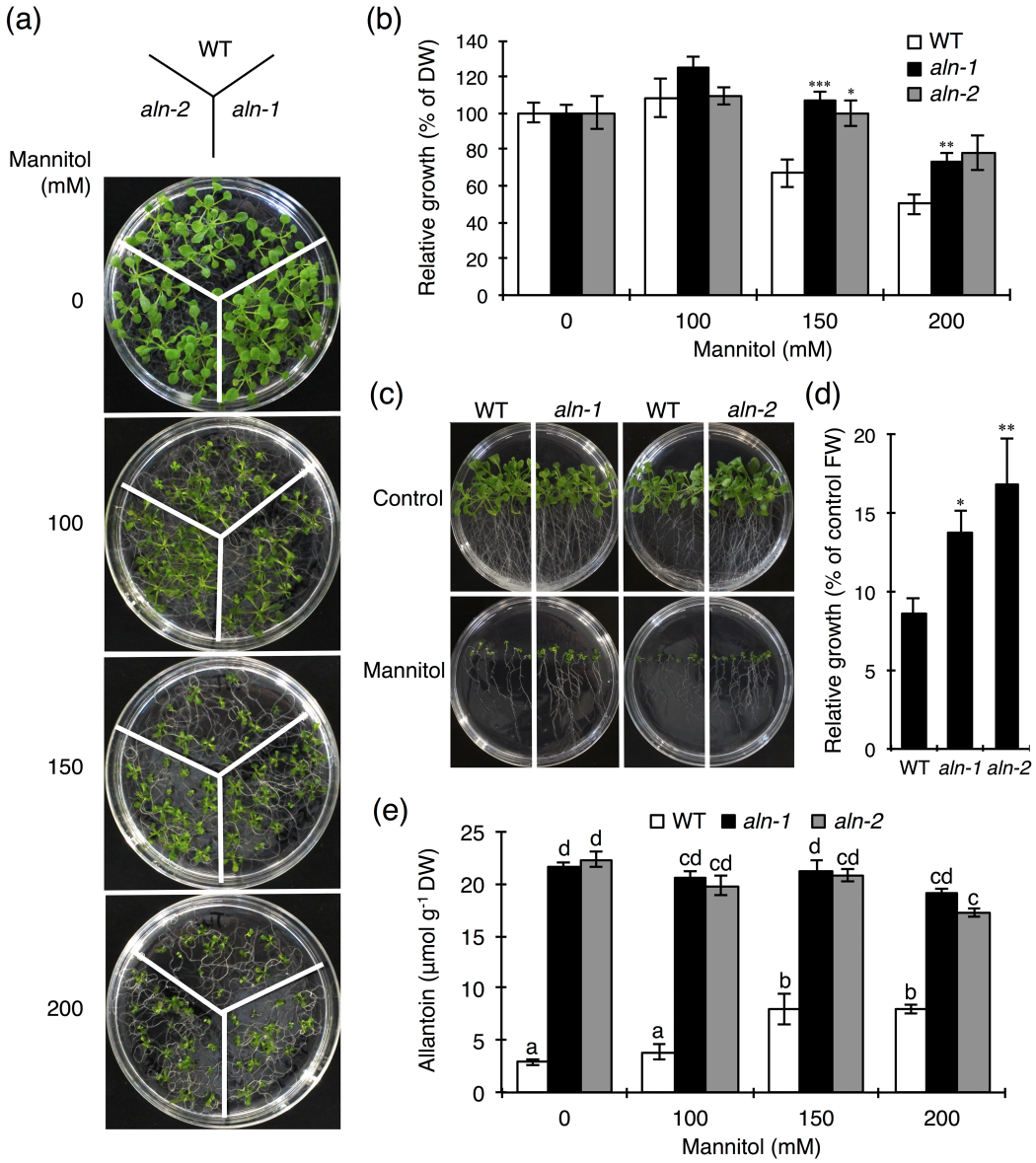

Figure I-8. Tolerance of *aln-1* and *aln-2* mutants to osmotic stress imposed by mannitol.

Seeds were germinated and grown for 14 days on standard medium supplemented with 100–200 mM mannitol (a, b, e) or, alternatively, 3-day-old seedlings were transferred onto standard medium containing 200 mM mannitol and grown for 14 days (c, d). Growth phenotype (a, c), relative growth (b, d) and allantoin level (e) of each genotype are shown. FW, fresh weight; DW, dry weight. The results are the mean of three independent experiments ± SEM (*$P < 0.05$, **$P < 0.01$, ***$P < 0.001$). Different letters in (e) indicate significant difference by one-way ANOVA with Tukey-Kramer's test ($P < 0.05$).

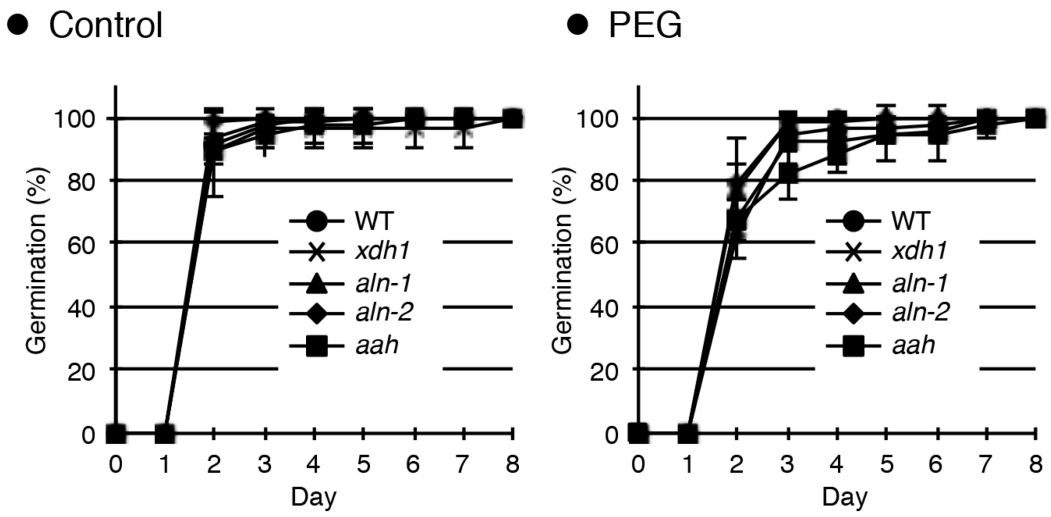

Figure I-9. Effects of osmotic stress imposed by PEG on seed germination of WT and the four purine-catabolic mutants.

The 1/2MS-agar plates were infused with PEG 8000 to reduce water potential (approximately –0.5 MPa), according to Verslues *et al*. (2006). Results are the mean of three independent experiments ± SEM.

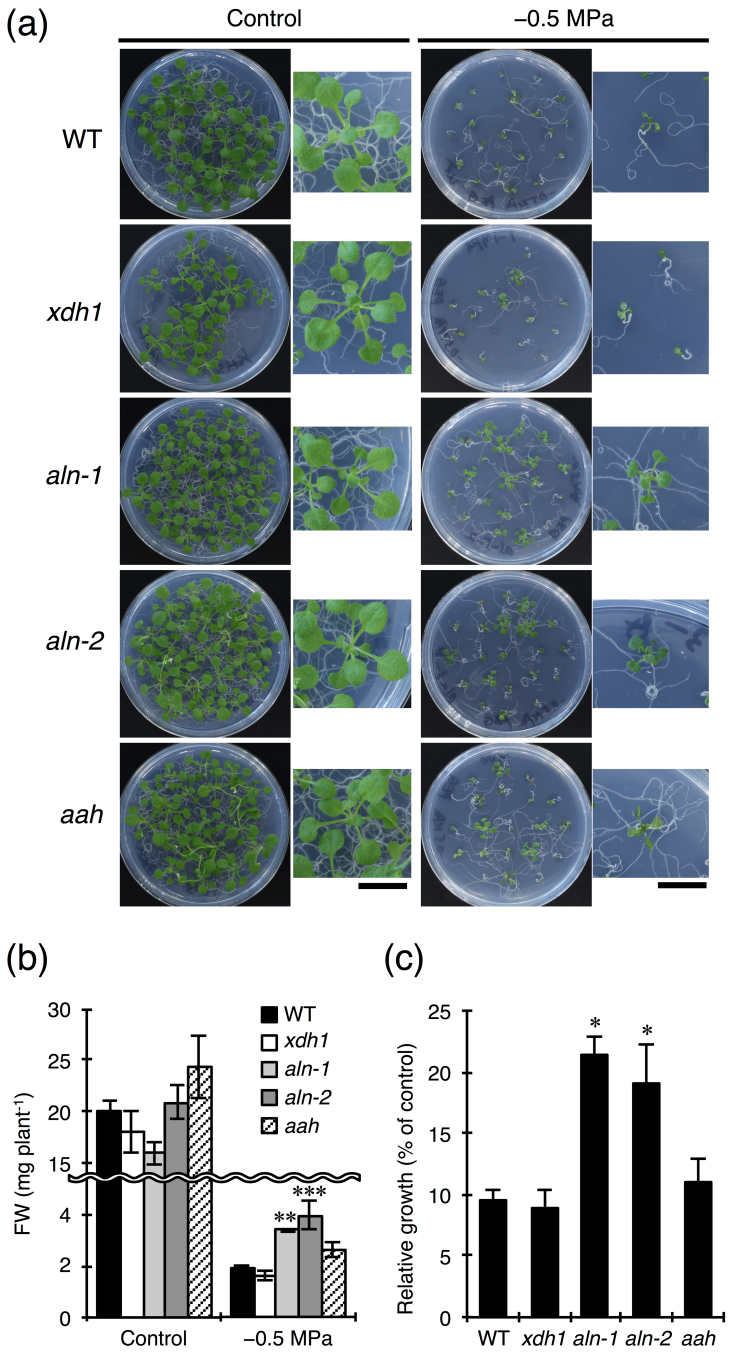

Figure I-10. Tolerance of *aln-1* and *aln-2* mutants to PEG-mediated osmotic stress. Seeds from WT and the four purine-catabolic mutants (*xdh1*, *aln-1*, *aln-2* and *aah*) were germinated and grown for 27 days on PEG-infused agar plates (–0.5 MPa). Growth phenotype (a), fresh weight (b), and relative growth (c) of each genotype are shown. Shown right of each picture in (a) is close-up image of representative plant growth (bar = 1 cm). FW, fresh weight. The results are the mean of three independent experiments ± SEM (*$P < 0.05$, **$P < 0.01$, ***$P < 0.001$).

CHAPTER II

Molecular and Physiological Analysis of the Role of Allantoin in Stress Acclimation of Arabidopsis

Introduction

The ureide allantoin is best known in plant biology as a key molecule in the transport and storage of symbiotically fixed nitrogen in tropical legumes like soybean (Schubert 1986; Smith and Atkins 2002). By contrast, the role of this ureide compound is unclear in non-leguminous species such as Arabidopsis and rice, except being a metabolic intermediate of purine catabolism. Recently, several research papers have reported that allantoin is a staple purine metabolite when plants are exposed to various forms of environmental stress such as drought and high salinity (Sagi *et al*. 1998; Nikiforova *et al*. 2005; Brychkova *et al*. 2008; Alamillo *et al*. 2010; Kanani *et al*. 2010; Rose *et al*. 2012). Therefore, allantoin is currently implicated in plant responses and adaptation to abiotic stress.

Despite the potential importance of allantoin in plant defense against stress, it still remains largely unknown how it contributes to stress protection, since the attempts to define the precise role has so far been limited to exogenous administration experiments. Such physiological studies using root tips or leaf discs have suggested that allantoin could protect plants from oxidative stress possibly by scavenging reactive oxygen species (ROS), because the pretreatment with allantoin effectively suppressed the appearance of damaging symptoms caused by ROS

(Gus'kov *et al*. 2004; Brychkova *et al*. 2008). However, the amounts of allantoin are generally low in plants, even under stress conditions (for example, below 1 μmol g^{-1} fresh weight in Arabidopsis; Brychkova *et al*. 2008), when compared to major antioxidants such as ascorbic acid. Moreover, *in vitro* assessment of antioxidant capacity argues against such a possibility (Wang *et al*. 2012). Thus, there is an obvious need to investigate the possible mechanisms of action of allantoin in plant acclimatization to abiotic stress.

In the previous chapter, I showed that the Arabidopsis mutants (*aln*) that accumulate allantoin enhanced drought and osmotic stress tolerance in Arabidopsis. Acclimation to stress environments involves reprogramming of gene expression at a genome-wide scale, which often results in the up-regulation of a large number of stress-associated or stress-responsive genes. Therefore, in this chapter, I examined the possible effect of allantoin accumulation on global-scale gene expression in Arabidopsis, by applying microarray analysis to the *aln-1* mutant. The results of transcriptome profiling and quantitative gene expression analyses of the *aln-1* mutant indicated that allantoin accumulation strongly affected ABA-responsive gene expression. Therefore, I also conducted the physiological experiments to address why allantoin could induce ABA responses under normal growth conditions, by examining the effect of its accumulation on ABA homeostasis and signaling.

Materials and Methods

Plant materials and growth conditions

The plant materials and growth conditions are described in CHAPTER I. To examine the effect of exogenously supplied allantoin, aseptically grown 12-day-old WT seedlings were transferred onto solid standard medium supplemented with various concentrations of allantoin and grown for 2 more days.

qRT-PCR

The procedures for RNA extraction and the method to quantify target transcript amounts by qRT-PCR are described in CHAPTER I. Gene-specific PCR primer sequences are listed in Table I-1. Relative gene expression data were analyzed using the comparative $2^{-\Delta\Delta Ct}$ method (Livak and Schmittgen 2001) after normalization with *ACT2* as the control transcript.

Microarray analysis

Total RNA was extracted from 2-week-old WT and *aln-1* seedlings as described above. Two independent biological samples were used per genotype. Target labeling and hybridization to Affymetrix ATH1 GeneChips were performed according to the manufacturer's instructions at the Analysis Center of Life Science, Hiroshima University. Hybridization signals were acquired using an Affymetrix GeneChip Scanner 3000 7G;

raw array images were analyzed using the MAS5 algorithm in GeneSpring GX software version 12 (Agilent Technology) to normalize probe sets. At the gene enumeration steps, control probe sets, ambiguous probe sets that were mapped to no or multiple loci in the TAIR10 genome annotation (http://www.arabidopsis.org), and probes for organelle-encoding genes were removed, while redundant probe sets representing the same locus were counted only once. Genes of interest were classified into functional categories using the Munich Information Center for Protein Sequences (MIPS) Functional Catalog *Arabidopsis* Database (Ruepp *et al*. 2004; http://mips.helmholtz-muenchen.de/proj/funcatDB/). The data reported in this paper have been deposited in the Gene Expression Omnibus (GEO) database, www.ncbi.nlm.nih.gov/geo (accession no. GSE44922).

Measurement of stomatal apertures

Stomatal aperture was measured by microscopy of a leaf epidermal strip. To prepare epidermal samples, the adaxial side of each leaf was stuck to transparent adhesive tape, and the epidermal layer was peeled from the abaxial side with another strip of adhesive tape. The resulting epidermal strips were examined for stomatal size by optical microscopy (Eclipse 80i; Nikon). Stomatal responses to ABA were examined according to Pei *et al*. (1997) with slight modification. Detached leaves were floated on 10 mM 2-(*N*-morpholino)-ethanesulfonic acid buffer (pH 6.5) containing 50 mM KCl and 0.1 mM $CaCl_2$ for 2 h under continuous light to ensure that stomata were open. After an additional incubation for 3 h in the presence or absence of ABA, widths of stomatal apertures were determined as described above.

Determination of ABA

The levels of free ABA were measured using an enzyme-linked immunosorbent assay (ELISA) as described previously (Dietz *et al*. 2000; Yan *et al*. 2007). Aerial parts of 2-week-old plants were ground in liquid nitrogen to a fine powder. Ground tissues were suspended in 80% (v/v) methanol containing 0.5 g l^{-1} citric acid monohydrate and 100 mg l^{-1} dibutylhydroxytoluene, and stirred overnight in the dark at 4ºC. The suspension was cleared by centrifugation at 1,000 × *g* for 20 min, and the supernatant was dried under vacuum. The resulting solid residue was dissolved in absolute methanol and added to TBS in a 1:9 volume ratio to measure free ABA. ELISA-based quantification was performed using the ABA Immunoassay detection kit (Sigma-Aldrich) according to the provided protocol.

Statistical analysis

All results are presented as means and SEM. The statistical evaluation was performed as described in CHAPTER I.

Results

aln *mutation causes genome-wide up-regulation of stress-related genes*

To determine the effect of *aln* mutation on genome-wide gene expression and to correlate these effects with the stress-tolerant *aln* phenotype, I performed comparative transcript-profiling with the Affymetrix ATH1 GeneChip using 2-week-old WT and *aln-1* mutant seedlings grown under normal, sterile conditions. Standard analysis of the microarray data using the Affymetrix protocols and GeneSpring software revealed that 1705 genes (988 up-regulated, 717 down-regulated) showed at least a 2.0-fold change in transcript levels between WT and the mutant. Increasing the cut-off threshold to 3.0-fold resulted in 545 genes (361 up-regulated, 184 down-regulated) displaying altered transcription in the *aln-1* mutant. Tables II-1 and II-2 summarize top 50 genes that were most significantly up-regulated and down-regulated in the *aln-1* mutant, respectively.

I classified the 361 up-regulated genes with at least a 3.0-fold change according to the top hierarchical level of functional categories described by the MIPS *Arabidopsis* Database (Ruepp *et al*. 2004). The significantly overrepresented genes (hypergeometric distribution: $P < 0.01$) were grouped into 5 functional categories (Fig. II-1a); most were relevant to stress response and adaptation, such as "Cell rescue, defense and virulence" ($P = 5.99 \times 10^{-13}$), "Systemic interaction with the environment" ($P = 1.54 \times 10^{-7}$), and "Interaction with the environment" ($P = 6.39 \times 10^{-6}$). Further classification at the lower levels of the MIPS functional catalogue revealed that genes assigned to functional subcategories "Osmotic and salt stress

response", "Osmosensing and response", "Abscisic acid response", and "Stress response" were among the most significantly overrepresented up-regulated genes (Table II-3).

Both aln *mutation and exogenous allantoin administration up-regulate stress/ABA-responsive gene expression*

I validated the microarray data by qRT-PCR to analyze expression of the five most up-regulated genes in our microarray experiments (Fig. II-2). To gain insights into the mechanisms underlying enhanced stress tolerance in *aln* seedlings, I quantified the expression of four representative genes that are induced by ABA as well as by osmotic and drought stress (*RD29A*, *RD29B*, *RD26*, and *COR15A*) (Fig. II-1b). As expected from the microarray data, the transcript levels of these stress-inducible genes were 2- to 16-fold higher in the *aln-1* mutant than in WT plants under normal growth conditions. However, restoring allantoin metabolism by genetic complementation totally abolished the enhanced expression of these genes exhibited by this mutant (Fig. II-1b). Moreover, neither *xdh1* nor *aah* mutants showed increased levels of these transcripts relative to WT expression (Fig. II-1c). These results suggest that the elevated allantoin levels might trigger ABA/stress-responsive gene expression without stress. To explore this possibility, the expression levels of *RD29A*, *RD29B*, and *RD26* were quantified in sterile WT seedlings after treatment for 2 days with various allantoin concentrations. Exogenously supplied allantoin induced expression of these genes in a dose-dependent manner (Fig. II-1d). Overall, these gene expression analyses indicate that allantoin or its

accumulation evokes osmotic and drought stress responses at the gene expression level in Arabidopsis under non-stress conditions.

aln *mutation increases ABA levels but does not alter the responses to ABA*

To examine the possible involvement of ABA in the enhanced stress tolerance and up-regulated expression of ABA/stress-responsive genes in *aln* mutants, I measured the levels of ABA in 2-week-old sterile seedlings of WT, *aln-1*, *xdh1* and *aah* genotypes grown under normal conditions. Compared to WT seedlings, only the *aln-1* mutant showed significantly increased ABA contents among the three purine-catabolic mutants (Fig. II-3a). Along with the enhanced ABA levels, the *aln-1* mutant had smaller stomatal apertures than did WT and *aah* mutants (Fig. II-3b). However, stomata of detached *aln-1* leaves responded similarly as those of WT and *aah* leaves to increased concentrations of external ABA (Fig. II-3c). Moreover, exogenous ABA induced ABA/stress-responsive gene expression in both *aln-1* and *aln-2* mutants at comparable levels to WT (Fig. II-3d). These results suggest that the *aln* mutation mainly influences ABA metabolism but does not significantly change the sensitivity or responses to ABA.

Discussion

How allantoin contributes to stress protection has been largely unexplored until now. Allantoin has been proposed to function as an antioxidant from a few studies showing that exogenous allantoin effectively mitigated oxidative damage when administered to roots or leaf discs (Gus'kov *et al*. 2004; Brychkova *et al*. 2008). Consistent with this assumption, genetically silencing purine degradation, which decreased allantoin levels, resulted in increased H_2O_2 in transgenic Arabidopsis (Brychkova *et al*. 2008; Watanabe *et al*. 2010). However, allantoin reportedly had no direct effect *in vitro* on quenching free radicals and inhibiting lipid peroxidation (Wang *et al*. 2012). Thus, whether this particular ureide compound exerts a direct effect *in vivo* as an efficient antioxidant awaits further physiological and biochemical examination.

Apart from the above possibility, we propose another hypothesis for the role of allantoin in the acquisition of stress tolerance. The remarkable aspects of the *aln* phenotype include global changes in transcript profiles with the significant up-regulation of stress-related genes, elevated ABA levels (Figs. II-1 to II-3). It is less likely that the *aln* mutation modified ABA signaling because the responses to exogenous ABA showed little difference between WT and the *aln* mutants (Fig. II-3c, d). These observations strongly indicate that the *aln* mutant is primed for stress responses probably through enhancing basal ABA levels (Fig. II-3a). Allantoin is very likely responsible for the observed priming effects because most of the aforementioned phenomena were reproduced by treating WT plants with this ureide, suggesting that its possible role in stress protection is regulatory, rather than functional as proposed

previously. This may explain why its antioxidant capacity was observed *in vivo* (Gus'kov *et al*. 2004; Brychkova *et al*. 2008) but not demonstrated *in vitro* (Wang *et al*. 2012). As shown in the previous chapter, the *aln* mutants accumulated allantoin constitutively, as opposed to inducible accumulation in WT plants, but had significantly higher concentrations under both stress and non-stress conditions (Figs. I-5e & I-8e). The stress-primed phenotype of the *aln* mutants suggests that there may be a certain threshold concentration above which allantoin could persistently evoke a key process of activating stress responses, such as accelerating ABA production. Consequently, we infer that, in the *aln* mutants, allantoin already exceeds such a threshold level under normal conditions while it does not reach the critical level in WT in our experimental conditions, unless supplied exogenously.

Recent studies on comparative plant physiology and metabolomics indeed imply the possibility of such a priming role for allantoin. For example, when two closely related species of *Sporobolu*s grass with highly contrasting desiccation tolerance are compared for their metabolome composition, even in the fully hydrated state, the tolerant species accumulates higher levels of osmolytes and other putative protective compounds including allantoin, suggesting that the plant is primed metabolically for drought stress (Oliver *et al*. 2011). Among rice cultivars of 15 different genotypes, there is a positive correlation between seed allantoin content and seedling survival under cold or dehydration conditions (Wang *et al*. 2012). More importantly, seed priming with allantoin significantly improves the early growth of a rice cultivar that accumulates poorly endogenous allantoin (Wang *et al*. 2012). These studies, together with the results presented in this thesis, strongly suggest the

previously unrecognized, possibly regulatory function of allantoin in the mechanism of stress tolerance of plants.

Table II-1. List of top 50 up-regulated genes in the *aln-1* mutant

Affymetrix probe ID	AGI[a]	Gene Description[b]	Fold Change[c]	*P*-value[d]
264415_at	At1g43160	RAP2.6, related to AP2 6	42.04	0.019573042
262517_at	At1g17180	ATGSTU25, GSTU25, glutathione S-transferase TAU 25	40.42	0.016660808
249599_at	At5g37990	S-adenosyl-L-methionine-dependent methyltransferases superfamily protein	30.27	0.007204956
247360_at	At5g63450	CYP94B1, cytochrome P450, family 94, subfamily B, polypeptide 1	21.29	0.030686967
265119_at	At1g62570	FMO GS-OX4, flavin-monooxygenase glucosinolate S-oxygenase 4	21.21	0.00330085
248079_at	At5g55790	unknown protein; BEST Arabidopsis thaliana protein match is: unknown protein (TAIR:AT1G45163.1); Has 1807 Blast hits to 1807 proteins in 277 species: Archae - 0; Bacteria - 0; Metazoa - 736; Fungi - 347; Plants - 385; Viruses - 0; Other Eukaryotes - 339 (source: NCBI BLink).	15.82	0.015486644
248205_at	At5g54300	Protein of unknown function (DUF761)	15.47	0.022860032
249812_at	At5g23830	MD-2-related lipid recognition domain-containing protein	15.05	0.023403123
266271_at	At2g29440	ATGSTU6, GST24, GSTU6, glutathione S-transferase tau 6	14.04	0.042197343
249010_at	At5g44580	unknown protein; FUNCTIONS IN: molecular_function unknown; INVOLVED IN: biological_process unknown; LOCATED IN: endomembrane system; EXPRESSED IN: 18 plant structures; EXPRESSED DURING: 12 growth stages; BEST Arabidopsis thaliana protein match is: unknown protein (TAIR:AT5G44582.1); Has 30201 Blast hits to 17322 proteins in 780 species: Archae - 12; Bacteria - 1396; Metazoa - 17338; Fungi - 3422; Plants - 5037; Viruses - 0; Other Eukaryotes - 2996 (source: NCBI BLink).	13.94	0.001026497
250662_at	At5g07010	ATST2A, ST2A, sulfotransferase 2A	12.84	0.041300207
260744_at	At1g15010	unknown protein; BEST Arabidopsis thaliana protein match is: unknown protein (TAIR:AT2G01300.1); Has 71 Blast hits to 71 proteins in 13 species: Archae - 0; Bacteria - 2; Metazoa - 0; Fungi - 0; Plants - 69; Viruses - 0; Other Eukaryotes - 0 (source: NCBI BLink).	12.22	0.0422675
249567_at	At5g38020	S-adenosyl-L-methionine-dependent methyltransferases superfamily protein	12.15	0.033257995
248392_at	At5g52050	MATE efflux family protein	12.02	0.06667782

Table II-1. List of top 50 up-regulated genes in the *aln-1* mutant (continued)

Affymetrix probe ID	AGI[a]	Gene Description[b]	Fold Change[c]	*P*-value[d]
256114_at	At1g16850	unknown protein; FUNCTIONS IN: molecular_function unknown; INVOLVED IN: response to salt stress; LOCATED IN: endomembrane system; EXPRESSED IN: leaf apex, leaf whorl, male gametophyte, flower, leaf; EXPRESSED DURING: LP.06 six leaves visible, LP.04 four leaves visible, LP.10 ten leaves visible, petal differentiation and expansion stage, LP.08 eight leaves visible; BEST Arabidopsis thaliana protein match is: unknown protein (TAIR:AT5G64820.1); Has 24 Blast hits to 24 proteins in 6 species: Archae - 0; Bacteria - 0; Metazoa - 0; Fungi - 0; Plants - 24; Viruses - 0; Other Eukaryotes - 0 (source: NCBI BLink).	11.13	0.000616687
253259_at	At4g34410	RRTF1, redox responsive transcription factor 1	10.98	0.03478151
245169_at	At2g33220	GRIM-19 protein	10.86	0.000294996
245689_at	At5g04120	Phosphoglycerate mutase family protein	10.84	0.01516615
253104_at	At4g36010	Pathogenesis-related thaumatin superfamily protein	10.37	0.011372128
249216_at	At5g42240	scpl42, serine carboxypeptidase-like 42	10.33	0.007154638
266901_at	At2g34600	JAZ7, TIFY5B, jasmonate-zim-domain protein 7	10.29	0.019238211
255484_at	At4g02540	Cysteine/Histidine-rich C1 domain family protein	10.20	0.001671626
247175_at	At5g65280	GCL1, GCR2-like 1	9.99	0.030675665
249101_at	At5g43580	Serine protease inhibitor, potato inhibitor I-type family protein	9.94	0.04029176
247431_at	At5g62520	SRO5, similar to RCD one 5	9.89	0.12785009
245504_at	At4g15660	Thioredoxin superfamily protein	9.65	0.001965331
261919_at	At1g65980	TPX1, thioredoxin-dependent peroxidase 1	9.50	0.000380261
266246_at	At2g27690	CYP94C1, cytochrome P450, family 94, subfamily C, polypeptide 1	9.38	0.01018095
249614_at	At5g37300	WSD1, O-acyltransferase (WSD1-like) family protein	9.00	0.1125418
254809_at	At4g12410	SAUR-like auxin-responsive protein family	8.91	0.000825102
265698_at	At2g32160	S-adenosyl-L-methionine-dependent methyltransferases superfamily protein	8.77	0.001731835
263594_at	At2g01880	ATPAP7, PAP7, purple acid phosphatase 7	8.75	0.04511567

Table II-1. List of top 50 up-regulated genes in the *aln-1* mutant (continued)

Affymetrix probe ID	AGI[a]	Gene Description[b]	Fold Change[c]	*P*-value[d]
258893_at	At3g05660	AtRLP33, RLP33, receptor like protein 33	8.72	0.011419615
251229_at	At3g62740	BGLU7, beta glucosidase 7	8.55	0.01898133
249971_at	At5g19110	Eukaryotic aspartyl protease family protein	8.52	0.1744212
245713_at	At5g04370	NAMT1, S-adenosyl-L-methionine-dependent methyltransferases superfamily protein	8.50	0.03838256
263320_at	At2g47180	AtGolS1, GolS1, galactinol synthase 1	8.48	0.033875797
248954_at	At5g45420	Duplicated homeodomain-like superfamily protein	8.35	0.003543388
260012_at	At1g67865	unknown protein; BEST Arabidopsis thaliana protein match is: unknown protein (TAIR:AT1G67860.1); Has 13 Blast hits to 13 proteins in 2 species: Archae - 0; Bacteria - 0; Metazoa - 0; Fungi - 0; Plants - 13; Viruses - 0; Other Eukaryotes - 0 (source: NCBI BLink).	8.23	0.02244117
265111_at	At1g62510	Bifunctional inhibitor/lipid-transfer protein/seed storage 2S albumin superfamily protein	8.06	0.001600498
250648_at	At5g06760	LEA4-5, Late Embryogenesis Abundant 4-5	7.94	0.02089907
255527_at	At4g02360	Protein of unknown function, DUF538	7.84	0.004926018
259846_at	At1g72140	Major facilitator superfamily protein	7.64	0.043517046
248293_at	At5g53050	alpha/beta-Hydrolases superfamily protein	7.63	0.006162878
263083_at	At2g27190	ATPAP1, ATPAP12, PAP1, PAP12, purple acid phosphatase 12	7.59	0.007613192
245628_at	At1g56650	ATMYB75, MYB75, PAP1, SIAA1, production of anthocyanin pigment 1	7.51	0.031996187
266799_at	At2g22860	ATPSK2, PSK2, phytosulfokine 2 precursor	7.49	0.07046978
245749_at	At1g51090	Heavy metal transport/detoxification superfamily protein	7.37	0.009178466
254561_at	At4g19160	unknown protein; Has 30201 Blast hits to 17322 proteins in 780 species: Archae - 12; Bacteria - 1396; Metazoa - 17338; Fungi - 3422; Plants - 5037; Viruses - 0; Other Eukaryotes - 2996 (source: NCBI BLink).	7.33	0.000476528

[a]Arabidopsis Genome Initiative gene index (http://www.arabidopsis.org/portals/nomenclature/guidelines.jsp).
[b]Gene symbol and description as provided by TAIR (http://www.arabidopsis.org/).
[c]Mean of two replicate experiments (*aln-1* versus WT).
[d]*P*-velue determined by unpaired Student's *t*-test.

Table II-2. List of top 50 the down-regulated genes in the *aln-1* mutant

Affymetrix probe ID	AGI[a]	Gene Description[b]	Fold Change[c]	*P*-value[d]
259925_at	At1g75040	PR-5, PR5, pathogenesis-related gene 5	-45.33	0.035682745
263174_at	At1g54040	ESP, ESR, TASTY, epithiospecifier protein	-28.09	0.001471174
267546_at	At2g32680	AtRLP23, RLP23, receptor like protein 23	-27.55	0.011935857
250445_at	At5g10760	Eukaryotic aspartyl protease family protein	-25.02	0.010145232
262421_at	At1g50290	unknown protein; Has 2 Blast hits to 2 proteins in 1 species: Archae - 0; Bacteria - 0; Metazoa - 0; Fungi - 0; Plants - 2; Viruses - 0; Other Eukaryotes - 0 (source: NCBI BLink).	-24.15	0.001628947
255437_at	At4g03060	AOP2, AOP2 (ALKENYL HYDROXALKYL PRODUCING 2); oxidoreductase, acting on paired donors, with incorporation or reduction of molecular oxygen, 2-oxoglutarate as one donor, and incorporation of one atom each of oxygen into both donors	-23.95	0.007742854
265837_at	At2g14560	LURP1, Protein of unknown function (DUF567)	-20.11	0.100942746
261449_at	At1g21120	O-methyltransferase family protein	-19.63	0.024762886
263133_at	At1g78450	SOUL heme-binding family protein	-17.73	0.007807442
250476_at	At5g10140	AGL25, FLC, FLC, FLF, K-box region and MADS-box transcription factor family protein	-16.72	0.007769419
258028_at	At3g27473	Cysteine/Histidine-rich C1 domain family protein	-15.39	0.00570533
249777_at	At5g24210	alpha/beta-Hydrolases superfamily protein	-14.46	0.04484017
249052_at	At5g44420	LCR77, PDF1.2, PDF1.2A, plant defensin 1.2	-13.36	0.031183869
258016_at	At3g19350	MPC, maternally expressed pab C-terminal	-11.67	0.004292169
247684_at	At5g59670	Leucine-rich repeat protein kinase family protein	-11.35	0.061674565
255310_at	At4g04955	ALN, ATALN, allantoinase	-11.03	0.004322603
252549_at	At3g45860	CRK4, cysteine-rich RLK (RECEPTOR-like protein kinase) 4	-10.83	0.051251277
264513_at	At1g09420	G6PD4, glucose-6-phosphate dehydrogenase 4	-10.25	0.003395705
262382_at	At1g72920	Toll-Interleukin-Resistance (TIR) domain family protein	-10.17	0.023818031
251625_at	At3g57260	BG2, BGL2, PR-2, PR2, beta-1,3-glucanase 2	-9.99	0.06797515
248683_at	At5g48490	Bifunctional inhibitor/lipid-transfer protein/seed storage 2S albumin superfamily protein	-9.91	0.017766595
249645_at	At5g36910	THI2.2, thionin 2.2	-8.97	0.003828495

Table II-2. List of top 50 the down-regulated genes in the *aln-1* mutant (continued)

Affymetrix probe ID	AGI[a]	Gene Description[b]	Fold Change[c]	*P*-value[d]
254574_at	At4g19430	unknown protein; FUNCTIONS IN: molecular_function unknown; INVOLVED IN: biological_process unknown; LOCATED IN: chloroplast; EXPRESSED IN: 17 plant structures; EXPRESSED DURING: 13 growth stages; Has 30201 Blast hits to 17322 proteins in 780 species: Archae - 12; Bacteria - 1396; Metazoa - 17338; Fungi - 3422; Plants - 5037; Viruses - 0; Other Eukaryotes - 2996 (source: NCBI BLink).	-8.85	0.02492709
248062_at	At5g55450	Bifunctional inhibitor/lipid-transfer protein/seed storage 2S albumin superfamily protein	-8.72	0.008941016
260904_at	At1g02450	NIMIN-1, NIMIN1, NIM1-interacting 1	-8.24	0.03442283
249117_at	At5g43840	AT-HSFA6A, HSFA6A, heat shock transcription factor A6A	-7.95	0.15852094
246821_at	At5g26920	CBP60G, Cam-binding protein 60-like G	-7.54	0.03489679
262542_at	At1g34180	anac016, NAC016, NAC domain containing protein 16	-7.37	0.010130536
252417_at	At3g47480	Calcium-binding EF-hand family protein	-7.20	0.16162959
265063_at	At1g61500	S-locus lectin protein kinase family protein	-6.95	0.010942
263947_at	At2g35820	ureidoglycolate hydrolases	-6.94	0.043847337
245690_at	At5g04230	ATPAL3, PAL3, phenyl alanine ammonia-lyase 3	-6.91	0.062932186
260568_at	At2g43570	CHI, chitinase, putative	-6.78	0.11462144
248169_at	At5g54610	ANK, ankyrin	-6.73	0.0532035
265208_at	At2g36690	2-oxoglutarate (2OG) and Fe(II)-dependent oxygenase superfamily protein	-6.30	0.039450236
253945_at	At4g27050	F-box/RNI-like superfamily protein	-6.27	3.71E-04
257623_at	At3g26210	CYP71B23, cytochrome P450, family 71, subfamily B, polypeptide 23	-6.20	0.006182943
249481_at	At5g38900	Thioredoxin superfamily protein	-6.20	0.013152028
250063_at	At5g17880	CSA1, disease resistance protein (TIR-NBS-LRR class)	-6.07	0.007657813
258147_at	At3g18070	BGLU43, beta glucosidase 43	-6.06	0.008160826
258537_at	At3g04210	Disease resistance protein (TIR-NBS class)	-6.04	0.03766801
257382_at	At2g40750	ATWRKY54, WRKY54, WRKY DNA-binding protein 54	-5.94	0.02949572
245349_at	At4g16690	ATMES16, MES16, methyl esterase 16	-5.90	0.01405258
256603_at	At3g28270	Protein of unknown function (DUF677)	-5.83	9.73E-04
246293_at	At3g56710	SIB1, sigma factor binding protein 1	-5.62	0.013424104
260015_at	At1g67980	CCOAMT, caffeoyl-CoA 3-O-methyltransferase	-5.51	0.21657525
267569_at	At2g30790	PSBP-2, photosystem II subunit P-2	-5.50	0.01755144

Table II-2. List of top 50 the down-regulated genes in the *aln-1* mutant (continued)

Affymetrix probe ID	AGI[a]	Gene Description[b]	Fold Change[c]	*P*-value[d]
245038_at	At2g26560	PLA IIA, PLA2A, PLP2, PLP2, phospholipase A 2A	-5.32	0.023045516
253411_at	At4g32980	ATH1, homeobox gene 1	-4.97	0.04292378
255319_at	At4g04220	AtRLP46, RLP46, receptor like protein 46	-4.96	0.014534462

[a]Arabidopsis Genome Initiative gene index (http://www.arabidopsis.org/portals/nomenclature/guidelines.jsp).
[b]Gene symbol and description as provided by TAIR (http://www.arabidopsis.org/).
[c]Mean of two replicate experiments (*aln-1* versus WT).
[d]*P*-velue determined by unpaired Student's *t*-test.

Table II-3. Top 10 most significantly overrepresented functional subcategories in the *aln-1* mutant.

FunCat number[a]	Functional subcategory	Observed frequency (%)	Expected frequency (%)	*P*-value
32.01.03	Osmotic and salt stress response	5.00	0.72	1.60×10^{-10}
34.11.03.13	Osmosensing and response	5.00	0.73	2.03×10^{-10}
36.20.18.05	Abscisic acid response	4.16	0.56	2.42×10^{-10}
32.01	Stress response	9.44	2.92	2.49×10^{-10}
01.20	Secondary metabolism	6.11	1.49	3.34×10^{-8}
34.11.03	Chemoperception and response	8.88	2.95	3.98×10^{-8}
34.11.03.12	Water response	3.05	0.41	3.61×10^{-7}
34.11	Cellular sensing and response to external stimulus	11.9	5.24	4.51×10^{-7}
36.20.18	Plant hormonal regulation	6.11	2.07	7.48×10^{-6}
20.01	Transported compounds (substrates)	13.0	6.65	7.96×10^{-6}

The functional classification was performed for 361 genes that were at least 3.0-fold up-regulated in the *aln-1* mutant using the MIPS interface (http://mips.helmholtz-muenchen.de/proj/funcatDB/), and functional subcategories (after the second hierarchical level) were ranked by their *P*-values, which were determined by comparing the observed with the expected frequencies for each functional subcategories using the hypergeometric distribution method.

[a]Functional catalogue number assigned to each of MIPS functional subcategories.

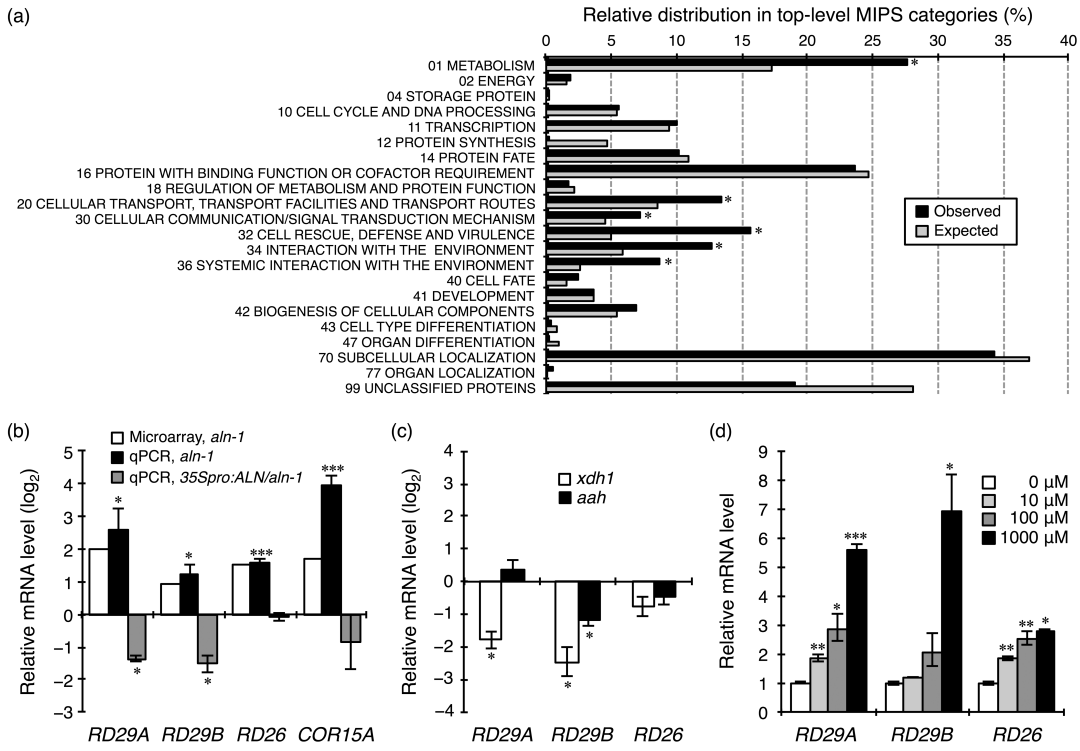

Figure II-1. Allantoin accumulation enhances ABA/stress-responsive gene expression.

(a) Functional classification of significantly up-regulated genes in the *aln-1* mutant. Genes up-regulated >3-fold in the *aln-1* mutant were classified according to the top-level functional categories of MIPS (Ruepp *et al*. 2004). Black bars indicate the distribution (%) of up-regulated genes and grey bars refer to the proportion (%) of Arabidopsis genes. Asterisks indicate that the distribution of up-regulated genes differs significantly from that of Arabidopsis genes (chi-square test, $P < 0.01$). (b, c) Transcript levels of typical stress/ABA-responsive genes in the *aln-1* mutant and *ALN/aln-1* complementation line (b), and in the *xdh1* and *aah* mutants (c). Levels of the selected mRNAs were determined by microarray or qRT-PCR, using total RNA from aerial parts of 2-week-old sterile plants grown under normal conditions. Shown are $\log_2$-transformed mRNA levels relative to WT. (d) Effects of exogenous allantoin on the expression of typical stress/ABA-responsive genes in WT plants. Results are the mean of three independent experiments ± SEM (*$P < 0.05$, **$P < 0.01$, ***$P < 0.001$).

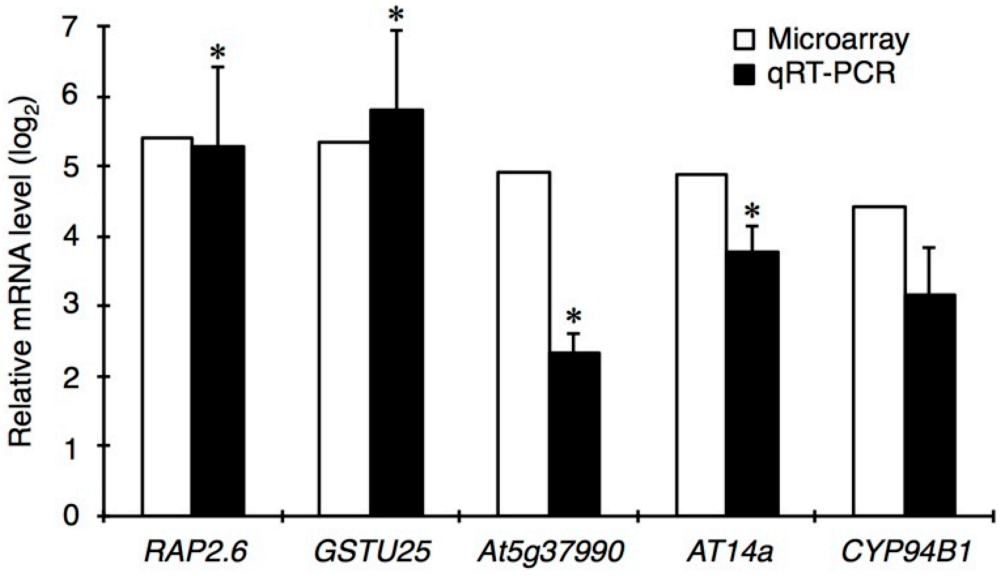

Figure II-2. Confirmation of the microarray expression data for the five most strongly up-regulated genes in the *aln-1* mutant by qRT-PCR.

mRNA levels for each gene in the *aln-1* mutant relative to WT (fold-change) were log2-transformed for microarray and qRT-PCR. Results are the mean of three independent experiments ± SEM (*$P < 0.05$ against WT).

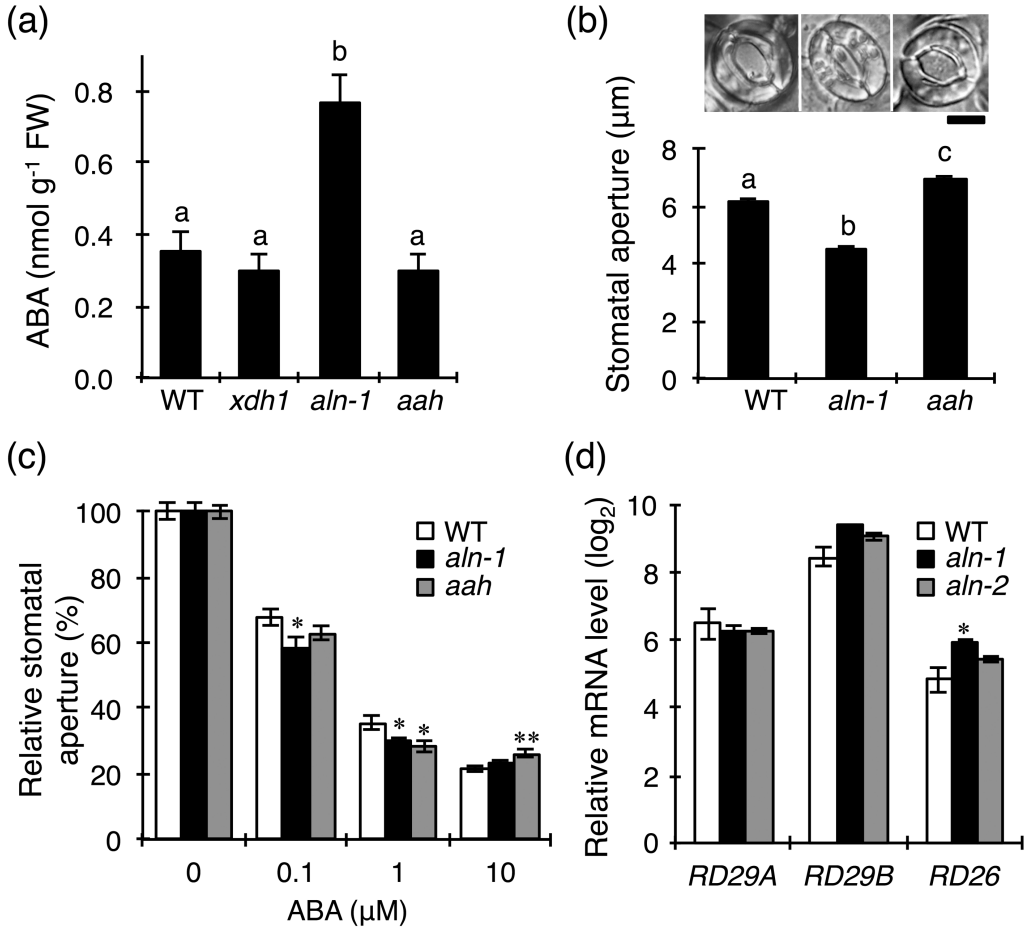

Figure II-3. Effects of the *aln* mutation on ABA levels, stomatal apertures, and responses to exogenous ABA.

(a) ABA levels in 2-week-old WT, *aln-1*, *xdh1* and *aah* seedlings grown under standard sterile conditions. (b) The average width of stomatal apertures for leaves of WT, *aln-1* and *aah* seedlings. Pictures show microscopy images of representative stomata (bar = 10 μm). (c) Stomatal responses to exogenous ABA in WT and two *aln* mutants. Detached leaves were floated on various concentrations of ABA and the widths of the stomatal apertures were measured. Levels are shown relative to the level in the control state (no ABA). (d) Effects of exogenous ABA on typical stress /ABA-responsive genes in WT and two *aln* mutants. Aseptically grown, 2-week-old seedlings were submerged in 100 μM ABA, and after 5-h incubation, total RNA was extracted to quantify the levels of *RD29A*, *RD29B* and *RD26* mRNAs by qRT-PCR. Results are the mean of three independent experiments ± SEM (**P* < 0.05, ***P* < 0.01). Different letters in (a, b) indicate significant difference by one-way ANOVA with Tukey's multiple comparison test (*P* < 0.05).

CHAPTER III

Molecular and Biochemical Analysis of the Mechanism by Which Allantoin Enhances ABA Levels

Introduction

ABA plays a central role in the responsiveness of plants to various kinds of environmental stresses, particularly drought and high salinity (Nambara and Marion-Poll 2005). ABA prevents water loss from the leaves by reducing transpiration through the regulation of stomatal aperture, and also modulates the expression patterns of more than 1000 genes (Seki *et al*. 2004). Levels of ABA can rapidly change in response to water status of cells and tissues, which is controlled by three metabolic processes, namely the *de novo* synthesis, deconjugation, and catabolism.

ABA is generated through the activation of two main pathways under stress conditions. One is the *de novo* pathway where five biosynthetic enzymes participate in the conversion from 9-*cis*-epoxycarotenoid to ABA, which is initiated in the plastids and ends in the cytosol. In Arabidopsis, the rate-limiting step in stress-induced ABA biosynthesis is the cleavage of carotenoids that is catalyzed by the plastid enzyme, 9-*cis*-epoxycarotenoid dioxygenase 3 (NCED3), whose expression is primarily regulated at the transcriptional level. The other pathway is the single-step deconjugation of inactive ABA conjugates that allows the liberation of free ABA, and this metabolic process has been recently reported to play a key role in rapid responses to abiotic stress (Lee *et al*. 2006; Wasilewska *et al*. 2008).

Among several inactive ABA conjugates, ABA-ß-D-glucosyl ester (ABA-GE) is the major compound. Hydrolysis of ABA-GE to release ABA is catalyzed by certain ß-glucosidases called BG1 (also known as BGLU18) and BG2 that are located in the ER and vacuole, respectively (Lee *et al*. 2006; Xu *et al*. 2012). The loss-of-function mutation of BG1 severely compromised a rapid and transient accumulation of ABA in response to drought stress in Arabidopsis, thereby causing drought hypersensitivity (Lee *et al*. 2006). Stress-mediated activation of BG1 mainly occurs post-translationally by multimerize monomer proteins into a highly polymerized complex. As for the degradation, the main catabolic step is 8'-hydroxylation of ABA, forming phaseic acid, which is further metabolized to dihydrophaseic acid. ABA 8'-hydroxylase is the rate-limiting enzyme in the catabolic process (Kushiro *et al.* 2004; Saito *et al*. 2004).

In CHAPTER II, I showed that allantoin accumulation resulted in activation of ABA-mediated stress responses at gene expression levels, such as the up-regulated expression of a number of stress/ABA-responsive genes. The stress responses mediated by allantoin were most likely caused by the enhanced basal ABA levels, suggesting that allantoin affects ABA metabolism. Thus, in this chapter, I investigated how allantoin could increase ABA levels using the *aln* mutant and WT plants that had been treated with exogenous allantoin. Specifically, I examined the effect of allantoin on the critical steps in ABA production, namely *NCED3* expression in the *de novo* biosynthesis and polymerization of BG1 in the deconjugation pathway.

Materials and Methods

Plant materials and growth conditions

The plant materials and growth conditions were essentially described in Chapters I and II. The seeds of *aba2-1* mutant (CS156; Léon-Kloosterziel *et al*. 1996) and the SALK T-DNA insertion line, *bglu18* (SALK_075731C; Ogasawara *et al*. 2009), which is disrupted in *BGLU18* (At1g52400; also known as *BG1*), were obtained from the Arabidopsis Biological Resource Center.

Promoter reporter assay

A 5'-upstream region (–1356 to + 125 bp relative to the transcription start site) of the gene encoding Arabidopsis NCED3 was obtained by PCR (for primers, see Table I-1), sequenced, and cloned into pUGW35 (Nakagawa *et al.* 2007b) to direct transcription of a firefly luciferase (Fluc) reporter gene. This plasmid was introduced into rosette leaves of 2-week-old seedlings by particle bombardment (PDU-1000/He, Bio-Rad), together with an internal control plasmid carrying a *Renilla reniformis* luciferase (Rluc) gene driven by the CaMV 35S promoter. The plants used were WT and *aln-1* mutants. Two days before bombardment, WT seedlings were transferred to 1/2MS medium containing allantoin at various concentrations. After bombardment, the plants were kept in the dark for 18 h before enzyme assay. Fluc and Rluc activities were measured using the Dual Luciferase Reporter Assay system (Promega) following the manufacturer's instructions. Chemiluminescence was recorded on a

microplate chemiluminometer (LB941, Berthold Technologies). The data obtained were expressed as Fluc activity normalized to Rluc activity.

Determination of ABA-glucose conjugate

For preparation of the hydrolyzable conjugate ABA-GE, the powdered tissues were lysed with 10 mM $CaCl_2$ for 24 h at 4ºC and centrifuged at 20,000 × *g* for 10 min. The supernatant was acidified to pH 3.0 with 0.1 M HCl and then extracted thrice with ethyl acetate to remove free ABA. The aqueous fractions containing ABA-GE were hydrolyzed with 1 M NaOH, after which the released ABA was acidified, partitioned into ethyl acetate, and dried as described in CHAPTER II. ELISA-based quantification was performed using the ABA Immunoassay detection kit (Sigma-Aldrich) according to the provided protocol.

Fractionation of native proteins by gel filtration column chromatography

Proteins were fractionated according to their native size by gel filtration column chromatography essentially as described previously (Lee *et al*. 2006). Aerial parts of 2-week-old plants were homogenized in 50 mM sodium phosphate buffer (pH 7.0) containing 150 mM NaCl, 0.02% (w/v) NaN_3, 10 mM dithiothreitol, and 0.1% (v/v) Triton X-100, and centrifuged twice at 14,000 × *g* at 4ºC for 10 min. After filtration through a membrane filter (DISMIC-13HP-PTFE*,* 0.45 μm pore size, Advantec), the supernatant was loaded onto a HiPrep16/60 Sephacryl S-300 high-resolution column using the ÄKTA*explorer* 10S system (GE Healthcare). For protein elution, the flow rate was adjusted to 0.5 ml min^{-1} and 3.0-ml fractions of effluent

were collected with the above buffer, without Triton X-100. An aliquot of each fraction was separated by SDS-PAGE using a 10% gel and transferred onto a PVDF membrane (Immobilon-P, Millipore). After blocking in 0.3% (w/v) skim milk, the blotted membrane was incubated with primary antibodies. The following antibodies were each used at 1:2000 dilution: anti-BG1/BGLU18 (Ogasawara *et al*. 2009), anti-glutamine synthetase (anti-GS; Sakamoto, Takeba and Tanaka 1990), and anti-nitrite reductase (anti-NiR; Shigeto *et al*. 2006). The membrane was then probed with anti-rabbit IgG secondary antibody conjugated to horseradish peroxidase (at 1:5000 dilution). Antigen-antibody complexes were detected in a chemiluminescence reaction using the Western Lighting Plus-ECL kit (Perkin-Elmer Life Sciences) and digitally captured on the VersaDoc 5000 imaging system using Quantity One software (Bio-Rad Laboratories).

Statistical analysis

All results are presented as means and SEM. The statistical evaluation was performed as described in CHAPTER I.

Results

Both aln *mutation and exogenous allantoin administration cause activation of the critical step in* de novo *ABA biosynthesis*

In Arabidopsis, two biochemical pathways are the source of the stress-induced ABA accumulation: *de novo* synthesis from plastid carotenoids and deconjugation of inactive ABA-GE to regenerate ABA (Nambara and Marion-Poll 2005). I asked whether either or both of these pathways were involved in the increased ABA levels in the *aln-1* mutant. Plastid-localized NCED is considered to be the rate-limiting enzyme in ABA biosynthesis in higher plants. In the *Arabidopsis* NCED family, NCED3 is responsible for drought-inducible ABA accumulation, which is essential for drought tolerance (Iuchi *et al*. 2001). The results of microarray and qRT-PCR showed that *NCED3* transcript levels increased by 3.9- and 2.4-fold, respectively, in the *aln-1* mutant compared to WT when 2-week-old seedlings were analyzed (Table II-1 and Fig. III-1). In contrast, *xdh1* and *aah* mutations had no significant effect on mRNA levels (Fig. III-1a). Elevated *NCED3* expression was also evident in WT seedlings after exposure to exogenous allantoin in the growth medium for 2 days (Fig. III-1b). Finally, when the *Fluc* reporter under control of the *NCED3* promoter was transiently expressed in 2-week-old plants, the dual-luciferase reporter assay revealed that the *NCED3* promoter was more active in the *aln-1* mutant than in WT (Fig. III-1c).

Both aln *mutation and exogenous allantoin administration cause activation of the critical step in the deconjugation of ABA-glucose conjugate*

The stress-induced increase in ABA is also mediated by the hydrolytic deconjugation of ABA-GE, which is catalyzed by BG1 (also known as BGLU18), an ER-localized ß-glucosidase (Lee *et al.* 2006). Under stress conditions, BG1 is activated through polymerization of the monomer enzyme to form a high molecular weight (MW) complex. I compared the degree of polymerization of BG1 in WT and *aln-1* to examine the involvement of the deconjugation route in the *aln* phenotype. Native protein extracts from 2-week-old seedlings were separated by gel filtration column chromatography and the fractions were subjected to immunoblotting to detect BG1 and other proteins of known MW (Fig. III-2a). Most BG1 existed predominantly as a monomer with the expected MW of 69,000 in sterile WT seedlings grown under normal conditions, and was converted into high MW forms upon drought shock. Surprisingly, normally grown *aln-1* seedlings displayed a broad distribution of BG1 in high MW fractions (more than 440,000) in addition to monomeric protein, indicating that a substantial proportion of BG1 from *aln-1* seedlings formed high MW complexes in the absence of stress. This upward shift in MW was unique to the *aln-1* mutant and hardly observed in *xdh1* and *aah* mutants. Also, the assembly of BG1 into high-MW forms was reproducible in non-stressed WT plants grown in the presence of allantoin (Fig. III-2a), supporting the idea that allantoin may be the cause of the polymerization of BG1. Consistent with the above observations, microsomal fractions from *aln-1* seedlings possessed 2.4-fold higher ABA-GE hydrolysis activity than fractions from WT (Fig. III-2b). Although compared to WT, the steady-state ABA-GE levels decreased only slightly, the ratio of ABA-GE/ABA was much lower in the *aln-1* mutant (Fig. III-2c, d).

aln *mutation affects the critical step in ABA catabolism*

Controlling the accumulation of ABA also involves the catabolic process (Nambara and Marion-Poll 2005). I therefore examined the transcript levels of members of the *CYP707A* family (*CYP707A1 – CYP707A4*) encoding ABA 8'-hydroxylases, the enzymes catalyzing the committed step in ABA degradation to phaseic acid. qRT-PCR revealed that *CYP707A* transcript levels were generally higher in the *aln-1* mutant, with the most up-regulated gene being *CYP707A1* (Fig. III-1d), possibly reflecting the elevated ABA level in this mutant because these catabolic genes are induced by ABA (Kushiro *et al.* 2004; Saito *et al*. 2004).

Taken together, these results show that elevated allantoin causes the synergistic activation of ABA metabolism, with the balance shifting towards increased ABA levels.

Exogenous allantoin increases ABA levels in WT, but not in mutants impaired in de novo *ABA biosynthesis and deconjugation of ABA-glucose conjugate*

To gain more insights into the mechanism by which allantoin enhanced the levels of and responses to ABA, I examined the effects of exogenous allantoin on ABA accumulation and the transcript levels of ABA/stress-responsive genes (*NCED3*, *RD29A*, *RD29B*, and *RD26*). I used WT and two ABA-related mutants, *aba2-1* and *bglu18*, which are impaired in the biochemical pathways leading to ABA production; specifically, *aba2-1* affects *de novo* ABA biosynthesis and *bglu18* affects

BG1-catalyzed deconjugation of ABA-glucose esters (Léon-Kloosterziel *et al*. 1996; Ogasawara *et al*. 2009). In WT seedlings, administration of allantoin significantly increased ABA levels by 2.5-fold (Fig. III-3a), with the concomitant up-regulation of the four typical ABA/stress-responsive genes (Fig. III-3b). In marked contrast to WT, the same treatment had no effect on either ABA accumulation or gene expression when applied to the two ABA-metabolic mutants. These results reveal that normal ABA production is required to elicit the *aln* phenotype in WT plants, indicating that allantoin evokes stress responses by affecting ABA levels.

Discussion

The results shown in CHAPTER II indicate that elevated allantoin levels cause the increases in cellular ABA levels, thereby priming ABA-mediated stress responses. This raises the critical issue of how allantoin enhances ABA levels. According to the current model, stress-induced ABA production occurs mainly through two pathways: *de novo* biosynthesis involving a set of plastidic and cytosolic enzymes including the rate-limiting NCED, and a simple one-step deconjugation reaction catalyzed by certain ß-glucosidases like BG1 allowing quick release of ABA from its inactive glucose conjugates. Under stress conditions, the former is activated by transcriptional induction of genes encoding biosynthetic enzymes while the latter requires post-translational activation of BG1 into a high MW complex (Cheng *et al*. 2002; Barrero *et al*. 2006; Lee *et al*. 2006). I therefore examined the effects of the *aln* mutation and exogenous allantoin on *NCED3* transcription and BG1 polymerization, the key steps in the respective routes for stress-induced ABA production. I found that, without exposure to stress, these two steps were activated to increase ABA levels in the *aln* mutant and also in WT plants when administered with exogenous allantoin (Figs. III-1 and III-2). However, the effect of allantoin on ABA production was abolished by either ABA-deficient *aba2-1* or BG1-knockout *bglu18* mutation (Fig. III-3). Of particular interest is that exogenous allantoin no longer activated *NCED3* expression in the *bglu18* mutant (Fig. III-3b), even though the *de novo* biosynthetic pathway remains intact in this mutant. The observation suggests that in normally grown *aln-1* mutant and allantoin-treated WT plants, transcriptional activation of *NCED3* may be mediated, at least in

part, by BG1 as illustrated in Figure III-4. Constitutively activated BG1 polymers can continually liberate ABA from ABA-GE, which would allow activation of ABA biosynthesis because *NCED3* expression is strongly induced by ABA (Cheng *et al*. 2002; Barrero *et al*. 2006). This mechanistic inference (Fig. III-4) conforms to the current model for positive feedback regulation of ABA biosynthesis (Xiong *et al*. 2002).

How allantoin can promote the polymerization of BG1 is another important question to be addressed. Although BG1 monomers polymerize for activation in response to drought (Lee *et al*. 2006; and this work Fig. III-2a), the molecular mechanism behind this remains largely unknown. We showed that both the endogenous allantoin accumulation in the *aln* mutant and exogenous allantoin application to WT brought about BG1 assembly into highly polymerized and enzymatically activated forms. Given that this enzyme is destined for the ER (Lee *et al*. 2006) where ureide metabolism occurs (Werner *et al*. 2008; see also Fig. I-1a), it is probable that allantoin is directly involved in the mechanism of BG1 activation in this particular subcellular compartment. An intriguing observation is that the elevated level of allantoate, the immediate metabolite of allantoin (Fig. I-1), failed to induce BG1 polymerization (Fig. III-2), suggesting that a certain specific interaction between BG1 and allantoin seems to lie in the basis of the possible mechanism. The nature of such possible interaction could be elucidated by *in vitro* experiments using recombinant BG1 proteins. In our experiments, the exogenous treatments with allantoin required rather high concentrations (100 to 1000 μM) to evoke ABA/stress-responsive gene expression or BG1 polymerization in WT plants. Assuming that co-localization of BG1 and allantoin may be critical for eliciting such stress responses, this may reflect the inefficiency

of the exogenous treatment in increasing allantoin at physiologically effective concentrations inside the ER. The presence of ureide transporters in the plasma membrane has been demonstrated in soybean (Collier and Tegeder 2012) and it is also likely in other plants including Arabidopsis (Schmidt *et al*. 2006). However, no equivalent transport systems are known to exist for inner membranes such as ER membranes.

The *aln* mutant simultaneously enhances expression of the family of ABA 8'-hydroxylases, the key enzyme in ABA catabolism (Fig. III-1d). This is an additional indication that the *aln* mutation has an impact on ABA metabolism because the ABA-dependent synergistic activation of the catabolic genes is considered to be part of the mechanism for precisely controlling ABA homeostasis (Kushiro *et al.* 2004; Saito *et al*. 2004). The results may also explain why the *aln* mutation causes increased ABA only at modest levels even though both the biosynthetic and deconjugation routes are activated in the mutant plants.

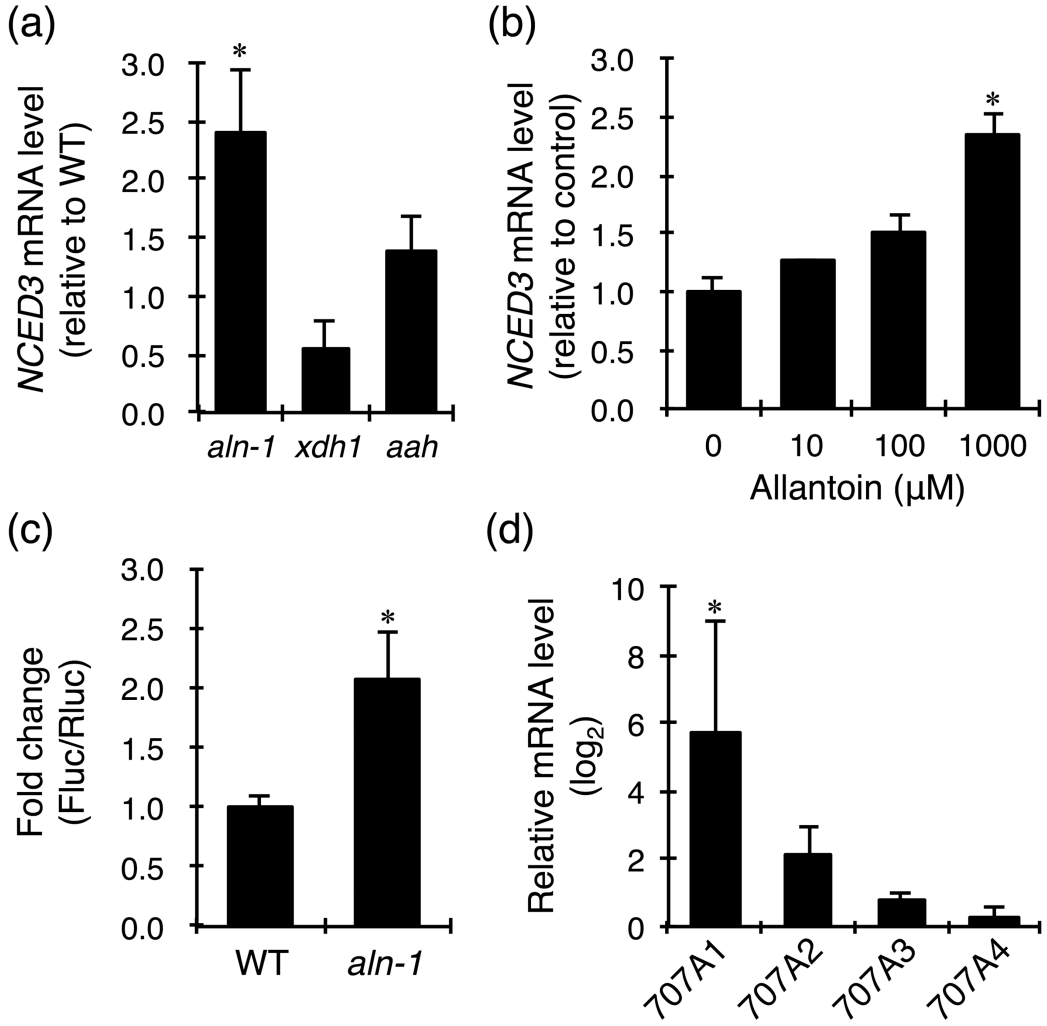

Figure III-1. Allantoin accumulation induces gene expression of the rate-limiting enzymes in *de novo* ABA synthesis and degradation.

(a) *NCED3* mRNA levels in 2-week-old, sterile seedlings of *aln-1*, *xdh1* and *aah* genotypes grown under normal conditions. (b) Effects of exogenous allantoin on *NCED3* expression in WT plants. *NCED3* transcripts were quantified as in Figure II-1d. (c) *NCED3* promoter activities in WT and *aln-1* mutant. Leaves from 2-week-old seedlings were bombarded with the *NCED3* promoter/*Fluc* fusion construct. After 18-h incubation, the promoter activity was measured by dual luciferase reporter assay. (d) Relative mRNA levels of the *CYP707A* family (*CYP707A1*, *CYP707A2*, *CYP707A3* and *CYP707A4*) in 2-week-old, sterile *aln-1* seedlings grown under normal conditions. Shown are $\log_2$-transformed mRNA levels relative to WT. Results are the mean of three independent experiments ± SEM (*$P < 0.05$).

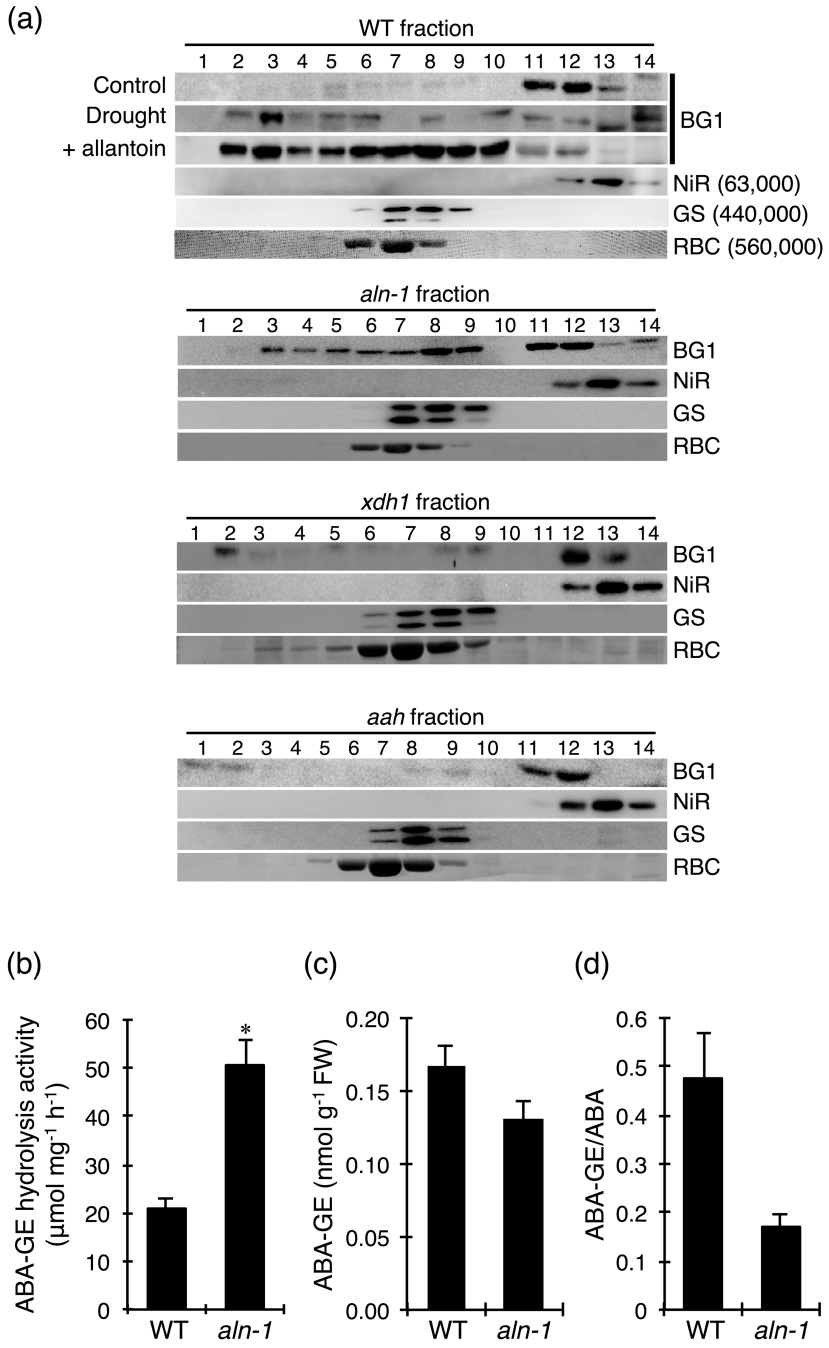

Figure III-2. Allantoin accumulation activates hydrolytic deconjugation of ABA-GE to liberate ABA.

(a) Molecular status of BG1 in WT, *aln-1, xdh1* and *aah* lines. Two-week-old sterile seedlings were used for protein extraction. Proteins were also sampled from age-matched WT seedlings after 3-h air-dry treatment (drought), or grown for 2 weeks with 100 µM allantoin (+ allantoin). Protein extracts were fractionated by gel filtration

column chromatography and each fraction was analyzed by immunoblotting after SDS-PAGE. Labeled on the right are immunologically detected or dye-stained proteins (GS, glutamine synthetase; NiR, nitrite reductase; RBC, ribulose-1,5-bisphosphate carboxylase) with native MW in parentheses, except for BG1, whose monomeric MW is ~69,000. The dual signals in GS detection correspond to plastid (upper) and cytosolic (lower) isoforms. The experiments were repeated at least twice with similar results. (b-d) ABA-GE hydrolysis activity (b), ABA-GE levels (c) and ABA-GE/ABA ratio (d) in 2-week-old, sterile WT and *aln-1* seedlings grown under normal conditions. Results are the mean of six (b) and three (c, d) independent experiments ± SEM (*$P < 0.05$).

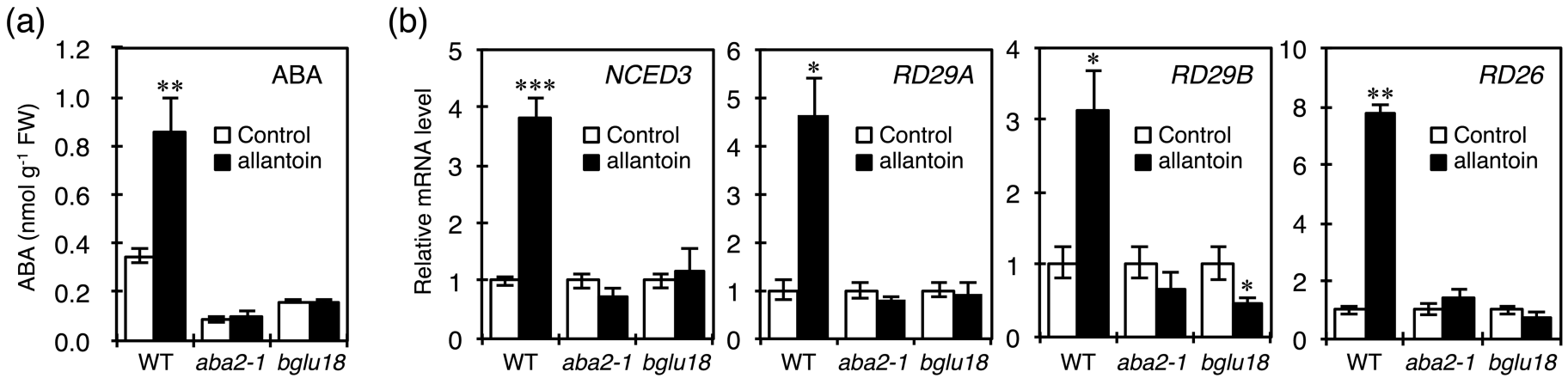

Figure III-3. Effects of exogenous allantoin on ABA levels and stress/ABA-responsive gene expression in WT plants and two ABA-metabolic mutants, *aba2-1* and *bglu18*.

(a) Endogenous ABA levels. (b) Relative mRNA levels of *NCED3*, *RD29A*, *RD29B* and *RD26*. Sterile seedlings of WT, *aba2-1* and *bglu18* were grown for 2 weeks on standard medium supplemented with 100 µM allantoin. Transcript amounts were quantified by qRT-PCR using total RNA extracted from aerial parts of the plants. FW, fresh weight. Results are the mean of three independent experiments ± SEM (**P* < 0.05, ***P* < 0.01, ****P* < 0.001).

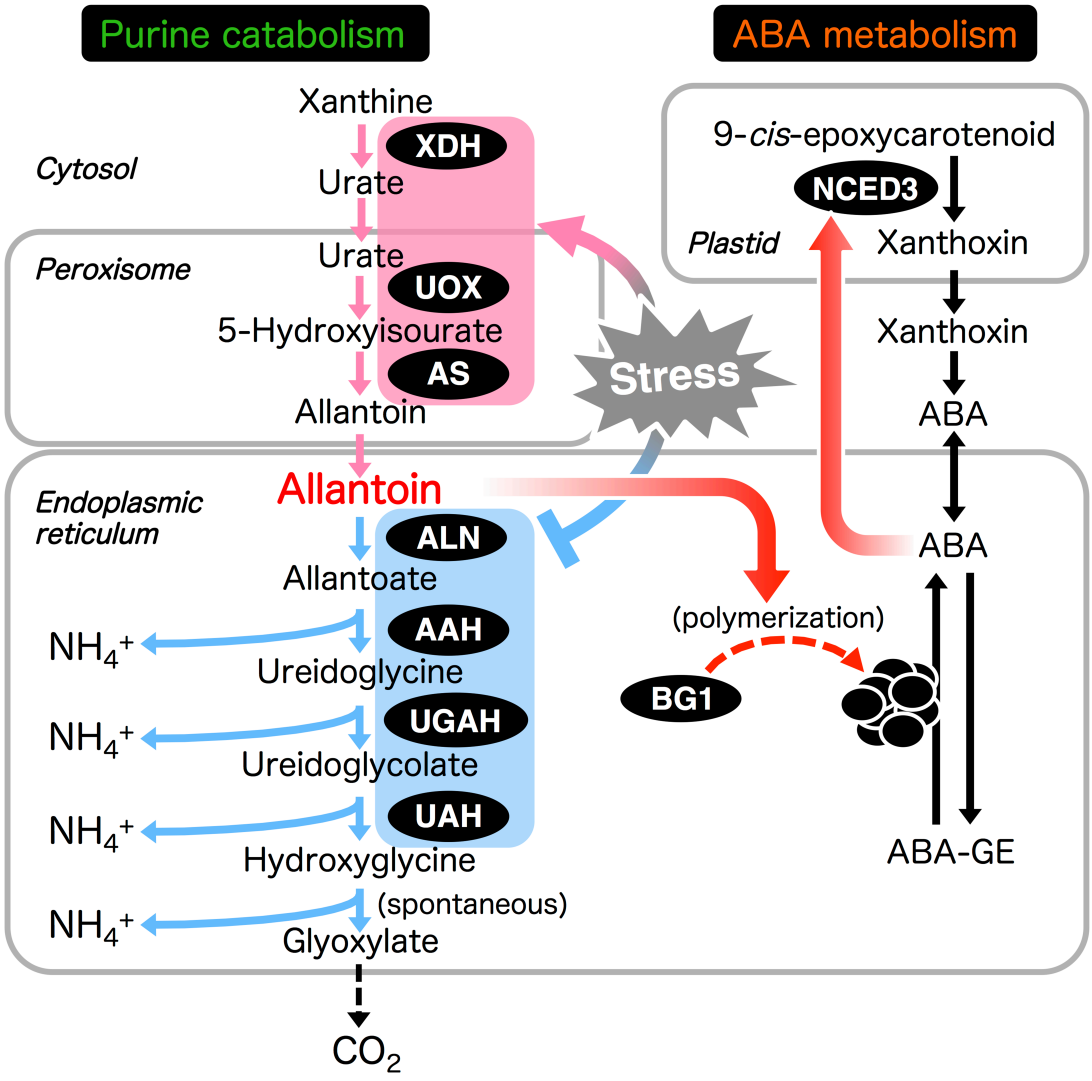

Figure III-4. Working hypothesis for the mechanism of allantoin-mediated activation of ABA production.

.

GENERAL CONCLUSIONS

In terrestrial plants, the catabolism of organic nitrogen allows a source-to-sink remobilization and recycling of nitrogen, which is essential for sustaining the growth, development and reproduction. Nucleobases, especially purine bases are considered a valuable source of remobilized nitrogen, since the complete breakdown of a purine ring, which proceeds through the intermediate formation of urate and allantoin, liberates four moles equivalent of ammonium that could be re-assimilated into amino acids (Zrenner *et al.* 2006). Apart from the aspect of nitrogen metabolism, recently, it has emerged that certain metabolic intermediates of purine degradation, such as allantoin, may be involved in stress protection of plants (Werner and Witte 2011). This possibility is supported by the recent reverse-genetic studies demonstrating that the purine metabolite deficiency causes the enhancement of stress sensitivity of transgenic Arabidopsis (Brychkova *et al*. 2008; Watanabe *et al.* 2010). However, it has remained to be elucidated how purine catabolism plays a role in or what purine metabolite contributes to protecting plants against stress. The main purpose of this study was to address these questions. Using reverse-genetic and molecular approaches, this study has provided several lines of evidence to support the importance of purine catabolism in stress protection of plants, with special emphasis on the critical role of the metabolic intermediate allantoin as described below. This study also demonstrates for the first time that genetically engineered alteration in purine catabolism can enhance stress tolerance of plants.

In CHAPTER I, by applying reverse-genetics to knockout three purine catabolic enzymes, XDH, ALN, and AAH, I showed that two allelic knockout mutations (*aln-1* and *aln-2*) in *ALN* specifically lead to enhanced growth and survival of Arabidopsis seedling under drought shock and osmotic stress conditions. I also demonstrated that, among the three metabolic mutants (*xdh1*, *aln* and *aah*) deficient in specific steps in purine degradation, only *aln* mutations induced allantoin accumulation that occurred consistently with increased stress tolerance. These results indicate that the stress-tolerant *aln* phenotype is not caused by a general response to purine catabolism inhibition, but rather results from a specific effect of allantoin, substantiating the importance of purine catabolism in stress tolerance. It is of note that, although one of the *aln* mutants (*aln-1*) was previously isolated, no distinguishable phenotypes were reported to be observed as compared to the WT plants (Yang and Han 2004).

In CHAPTER II, using a microarray-based approach, I revealed that the *aln* mutation causes genome-wide alterations in the levels of transcripts associated with stress responses and adaptation, with pronounced up-regulation of stress-inducible and ABA-regulated genes. Such changes in gene expression were not observed in either *xdh* or *aah* mutant, suggesting that allantoin may have the ability to activate ABA/stress-responsive gene expression. In order to explore this possibility, I treated WT plants with exogenous allantoin and examined whether typical stress/ABA-responsive genes are induced or not at the mRNA level. The results of qRT-PCR analysis showed that the transcript levels of these genes increased in allantoin-treated WT plants in the absence of stress. These results strongly suggest the potential of allantoin in modulating the

stress response at the level of gene expression, possibly by mediating the enhancement of cellular ABA levels. Indeed, as compared to WT, the *aln-1* mutant accumulated a 2-fold higher level of this stress hormone. However, the responses of the *aln* mutants to exogenously supplied ABA were hardly different from those of WT plants, suggesting that allantoin affects ABA metabolism rather than ABA signaling.

In CHAPTER III, using molecular and biochemical approaches, I attempted to elucidate how allantoin enhances intracellular ABA levels. The main pathways leading to ABA production are the *de novo* synthesis and deconjugation of ABA-glucose conjugate, both of which are activated under stress conditions. Therefore, I examined whether allantoin could activate the critical step in each pathway. I found that both *NCED3* transcription and BG1 polymerization were activated specifically by the *aln* mutation, but not by *xdh1* and *aah* mutations. Moreover, the exogenous allantoin reproducibly activated the two pathways causing the enhanced ABA accumulation in normally grown WT seedlings. Finally, the effect of exogenous allantoin was abolished by two mutations (*aba2-1* and *bglu18*) that are defective in the *de novo* biosynthesis and BG-mediated deconjugation reaction, respectively. These results clearly indicate that allantoin can enhance ABA levels through synergistic activation of the two main pathways leading to ABA production, suggesting the possible connection of purine degradation to ABA metabolism in the regulation of plant acclimatization to abiotic stress.

The results presented in this thesis suggest that allantoin degradation is a critical step of purine catabolism in plants under stress conditions.

Under normal growth conditions and during the developmental progression to leaf senescence, plant purine catabolism plays a housekeeping role and allantoin is further degraded for nitrogen recycling and mobilization (Stasolla *et al.* 2003; Zrenner *et al.* 2006; Werner and Witte 2011). The use of a housekeeping metabolic intermediate in stress response and adaptation may enable prompt responses to environmental changes; stress-induced inhibition of the catabolic enzyme or down-regulation of its gene expression allows temporary accumulation of the intermediate with protective or regulatory properties. In fact, analysis of publicly available Arabidopsis microarray data (Kilian *et al*. 2007) suggests that such transcriptional regulation is likely to occur in the drought response, because mRNA levels of purine-catabolic enzymes increase during normal leaf aging, but genes for these enzymes respond differentially to drought stress in an expression pattern that would result in allantoin accumulation (Fig. 2).

I hypothesized that plants could make effective use of purine catabolism for nutritional recycling or stress responses, depending on the physiological status and surrounding environmental conditions. Plants have evolved to diversify and expand their metabolism to compensate for their sessile nature, and such a dual function of a single metabolic pathway may endow plants with rapid, flexible, and less costly strategies for continued growth and survival in response to constantly changing environments or changes in nutrient availability.

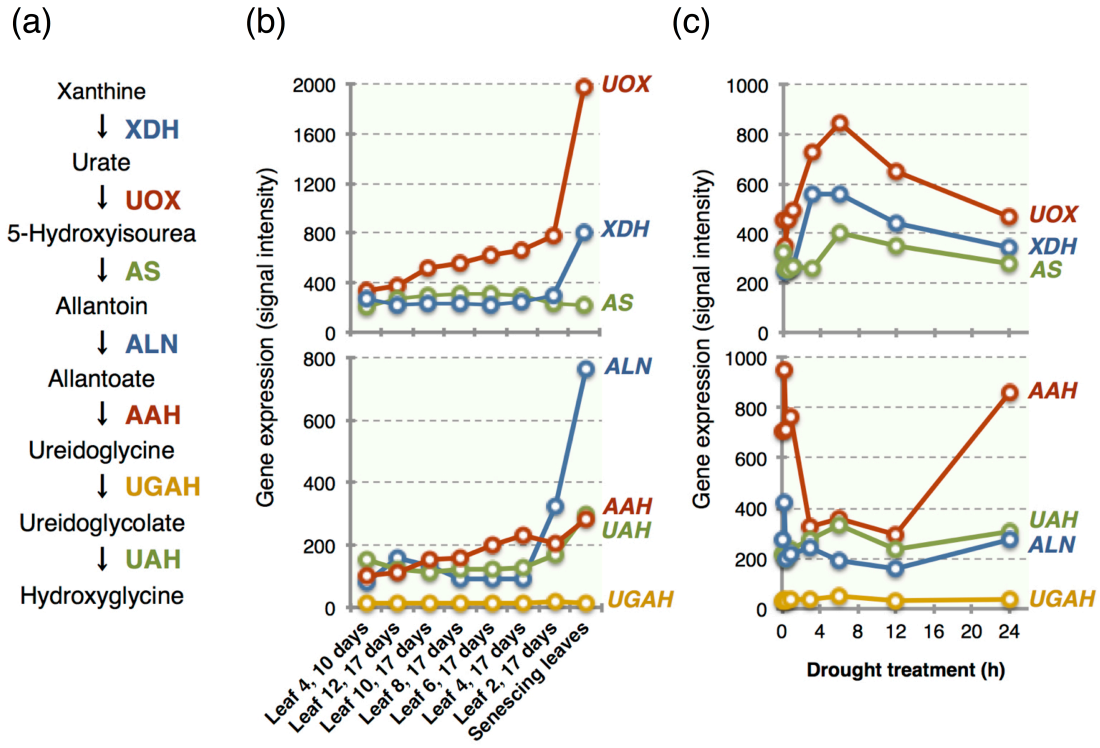

Figure 2. Coordinated and differential expression of purine catabolic enzymes in Arabidopsis.

(a) The purine catabolism pathway. For abbreviated enzyme names, see the legend of Figure 1 of General Introduction. (b and c) Transcript analysis of purine catabolic enzymes using publicly available gene expression profiles from AtGenExpress (http://www.Arabidopsis.org/info/expression/ATGenExpress.jsp). For clarity, transcript profiles are shown separately for the first and last half of the metabolic pathway: *upper*, transcripts encoding enzymes (XDH, UOX and AS) involved in xanthine oxidation to form allantoin; *lower*, transcripts encoding enzymes (ALN, AAH, UGAH, and UAH) for the ureide hydrolysis. (b) Transcripts for most enzymes in the pathway increase during natural leaf aging, particularly in senescing leaves. Such coordinated expression would allow efficient recycling of purine ring nitrogen from source to sink organs. (c) The two enzyme groups display a highly contrasting pattern of transcript abundance in response to drought. Such differentially regulated expression might promote xanthine degradation and prevent allantoin degradation, resulting in transient allantoin accumulation. Experimental data were obtained from 18-day-old WT Arabidopsis seedlings subjected to stress treatments (Kilian *et al*. 2007).

Acknowledgements

This study was carried out in Laboratory of Molecular Plant Biology, Department of Mathematical and Life Sciences, Graduate School of Science, Hiroshima University.

I would like to express my sincere appreciation to Professor Atsushi Sakamoto, Hiroshima University, for giving me the chance to perform this study, and for his patient guidance, discussion, invaluable suggestion and constant support.

I thank Professor Mikio Nishimura, National Institute for Basic Biology, for providing the BG1/BGLU18 antibody, Professor Tsuyosi Nakagawa, Shimane University, for providing the Gateway cloning vectors pGWB14 and pUGW35, and Associate Professor Tomokazu Konishi, Akita Prefectural University, for giving advice and discussing on microarray analysis. I also express my appreciation to Professor Shunsuke Izumi, Hiroshima University, for his kind help on determination of ABA. I wish to thank Associate Professor Hiroshi Shimada and Assistant Professor Misa Takahashi, Hiroshima University, and Dr. Ayami Nakagawa, ASAGIRI AGRICULTURE Co., Ltd., for their valuable advices, collaboration, and warm encouragements.

I am profoundly grateful to all past and current members of Laboratory of Molecular Plant Biology. Particularly, I thank Mses Yuka Kounosu, Satomi Maeda, Yu LV, Atsumi Yama and Mayumi Matsumoto, and Messrs. Takafumi Sugimoto, Kouya Kajimura, Hiroshi Takagi, Yuki Hakomori and Nobuhiro Akiyoshi, for their collaboration and technical assistance.

Finally, I would like to greatly appreciate my family and friends for their support and encouragement throughout my study.

This study was financially supported in part by a Grant-in-Aid for Research Fellow of Japan Society for the Promotion of Science (DC2, no. 23-7275).

References

Alamillo J.M., Diaz-Leal J.L., Sanchez-Moran M.V. and Pineda M. (2010) Molecular analysis of ureide accumulation under drought stress in *Phaseolus vulgaris* L. *Plant, Cell & Environment* **33**: 1828-1837.

Ashihara H. and Suzuki T. (2004) Distribution and biosynthesis of caffeine in plants. *Frontirs of Bioscience* **9**: 1864-1876.

Barrero J.M., Rodriguez P.L., Quesada V., Piqueras P., Ponce M.R. and Micol J.L. (2006) Both abscisic acid (ABA)-dependent and ABA-independent pathways govern the induction of *NCED3*, *AAO3* and *ABA1* in response to salt stress. *Plant, Cell & Environment* **29**: 2000-2008.

Brychkova G., Alikulov Z., Fluhr R. and Sagi M. (2008) A critical role for ureides in dark and senescence-induced purine remobilization is unmasked in the *Atxdh1* Arabidopsis mutant. *Plant Journal* **54**: 496-509.

Cheng W.H., Endo A., Zhou L., Penney J., Chen H.C., Arroyo A., Leon P., Nambara E., Asami T., Seo M., Koshiba T. and Sheen J. (2002) A unique short-chain dehydrogenase/reductase in Arabidopsis glucose signaling and abscisic acid biosynthesis and functions. *Plant Cell* **14**: 2723-2743.

Clough S.J. and Bent A.F. (1998) Floral dip: a simplified method for *Agrobacterium*-mediated transformation of *Arabidopsis thaliana*. *Plant Journal* **16**: 735-743.

Collier R. and Tegeder M. (2012) Soybean ureide transporters play a critical role in nodule development, function and nitrogen export. *Plant Journal* **72**: 355–367.

Crozier A., Kamiya Y., Bishop G. and Yokota T. (2000) Biosynthesis of hormones and elicitor molecules. In: Buchanan B.B., Gruissen W. and Jones R.L. (eds) *Biochemistry and Molecular Biology of Plants*. American Society of Plant Physiologists, Rockvill, Maryland pp 850-929.

Datta D.B., Triplett E.W. and Newcomb E.H. (1991) Localization of xanthine dehydrogenase in cowpea root nodules: implications for the interaction between cellular compartments during ureide biogenesis. *Proceedings of the National Academy of Sciences of the United States of America* **88**: 4700-4702.

Dietz K.J., Sauter A., Wichert K., Messdaghi D. and Hartung W. (2000) Extracellular ß-glucosidase activity in barley involved in the hydrolysis of ABA glucose conjugate in leaves. *Journal of Experimental Botany* **51**: 937-944.

Gus'kov E.P., Prokof'ev V.N., Kletskii M.E., Kornienko I.V., Gapurenko O.A., Olekhnovich L.P., Chistyakov V.A., Shestopalov A.V., Sazykina

M.A., Markeev A.V., Shkurat T.P., Malkhos'yan S.R. and Zhdanov Yu.A. (2004) Allantoin as a vitamin. *Doklady Biochemistry and Biophysics* **398**: 320–324.

Hayashi S., Fujiwara S. and Noguchi T. (2000) Evolution of urate-degrading enzymes in animal peroxisomes. *Cell Biochemistry and Biophysics* **32**: 123-129.

Hesberg C., Hansch R., Mendel R.R. and Bittner F. (2004) Tandem orientation of duplicated xanthine dehydrogenase genes from *Arabidopsis thaliana*: differential gene expression and enzyme activities. *Journal of Biological Chemistry* **279**: 13547-13554.

Iuchi S., Kobayashi M., Taji T., Naramoto M., Seki M., Kato T., Tabata S., Kakubari Y., Yamaguchi-Shinozaki K. and Shinozaki K. (2001) Regulation of drought tolerance by gene manipulation of 9-*cis*-epoxycarotenoid dioxygenase, a key enzyme in abscisic acid biosynthesis in *Arabidopsis*. *Plant Journal* **27**: 325-333.

Kanani H., Dutta B. and Klapa M.I. (2010) Individual vs. combinatorial effect of elevated CO_2 conditions and salinity stress on *Arabidopsis thaliana* liquid cultures: comparing the early molecular response using time-series transcriptomic and metabolomic analyses. *BMC Systems Biology* **4**: 177.

Kilian J., Whitehead D., Horak J., Wanke D., Weinl S., Batistic O., D'Angelo C., Bornberg-Bauer E., Kudla J. and Harter K. (2007) The

AtGenExpress global stress expression data set: protocols, evaluation and model data analysis of UV-B light, drought and cold stress responses. *Plant Journal* **50**: 347-363.

Kushiro T., Okamoto M., Nakabayashi K., Yamagishi K., Kitamura S., Asami T., Hirai N., Koshiba T., Kamiya Y. and Nambara E. (2004) The *Arabidopsis* cytochrome P450 CYP707A encodes ABA 8'-hydroxylases: key enzymes in ABA catabolism. *EMBO Journal* **23**: 1647-1656.

Lamberto I., Percudani R., Gatti R., Folli C. and Petrucco S. (2010) Conserved alternative splicing of *Arabidopsis* transthyretin-like determines protein localization and S-allantoin synthesis in peroxisomes. *Plant Cell* **22**: 1564-1574.

Lee K.H., Piao H.L., Kim H.Y., Choi S.M., Jiang F., Hartung W., Hwang I., Kwak J.M., Lee I.J. and Hwang I. (2006) Activation of glucosidase via stress-induced polymerization rapidly increases active pools of abscisic acid. *Cell* **126**: 1109-1120.

Leon-Kloosterziel K.M., Gil M.A., Ruijs G.J., Jacobsen S.E., Olszewski N.E., Schwartz S.H., Zeevaart J.A. and Koornneef M. (1996) Isolation and characterization of abscisic acid-deficient Arabidopsis mutants at two new loci. *Plant Journal* **10**: 655-661.

Livak K.J. and Schmittgen T.D. (2001) Analysis of Relative Gene Expression Data Using Real-Time Quantitative PCR and the $2^{-\Delta\Delta Ct}$ Method. *Methods* **25**: 402-408.

Moffatt B.A. and Ashihara H. (2002) Purine and pyrimidine nucleotide synthesis and metabolism. In: *Arabidopsis Book. 2nd Edition*, American Society of Plant Biologists, Rockville, MD, Online publication. DOI/10.1199/tab.0018 http://aspb.org/publications/arabidopsis/

Montalbini P. (1991) Effect of rust infection on levels of uricase, allantoinase and ureides in susceptible and hypersensitive bean leaves. *Physiological and Molecular Plant Pathology* **39**: 173-188.

Montalbini P. (1995) Effect of rust infection on purine catabolism enzyme levels in wheat leaves. *Physiological and Molecular Plant Pathology* **46**: 275-292.

Nakagawa A., Sakamoto S., Takahashi M., Morikawa H. and Sakamoto A. (2007) The RNAi-mediated silencing of xanthine dehydrogenase impairs growth and fertility and accelerates leaf senescence in transgenic Arabidopsis plants. *Plant and Cell Physiology* **48**: 1484-1495.

Nakagawa T., Kurose T., Hino T., Tanaka K., Kawamukai M., Niwa Y., Toyooka K., Matsuoka K., Jinbo T. and Kimura T. (2007) Development of series of gateway binary vectors, pGWBs, for realizing

efficient construction of fusion genes for plant transformation. *Journal of Bioscience and Bioengineering* **104**: 34-41.

Nambara E. and Marion-Poll A. (2005) Abscisic acid biosynthesis and catabolism. *Annual Review of Plant Biology* **56**: 165-185.

Nikiforova V.J., Kopka J., Tolstikov V., Fiehn O., Hopkins L., Hawkesford M.J., Hesse H. and Hoefgen R. (2005) Systems rebalancing of metabolism in response to sulfur deprivation, as revealed by metabolome analysis of Arabidopsis plants. *Plant Physiology* **138**: 304-318.

Ogasawara K., Yamada K., Christeller J.T., Kondo M., Hatsugai N., Hara-Nishimura I. and Nishimura M. (2009) Constitutive and inducible ER bodies of *Arabidopsis thaliana* accumulate distinct beta-glucosidases. *Plant and Cell Physiology* **50**: 480-488.

Oliver M.J., Guo L., Alexander D.C., Ryals J.A., Wone B.W. and Cushman J.C. (2011) A sister group contrast using untargeted global metabolomic analysis delineates the biochemical regulation underlying desiccation tolerance in *Sporobolus stapfianus*. *Plant Cell* **23**: 1231-1248.

Pei Z., Kuchitsu K., Ward J., Schwarz M. and Schroeder J. (1997) Differential abscisic acid regulation of guard cell slow anion channels in Arabidopsis wild-type and *abi1* and *abi2* mutants. *Plant Cell* **9**: 409-423.

Pessoa J., Sarkany Z., Ferreira-da-Silva F., Martins S., Almeida M.R., Li J. and Damas A.M. (2010) Functional characterization of *Arabidopsis thaliana* transthyretin-like protein. *BMC Plant Biology* **10**: 30.

Rose M.T., Rose T.J., Pariasca-Tanaka J., Yoshihashi T., Neuweger H., Goesmann A., Frei M. and Wissuwa M. (2012) Root metabolic response of rice (*Oryza sativa* L.) genotypes with contrasting tolerance to zinc deficiency and bicarbonate excess. *Planta* **236**: 959-973.

Ruepp A., Zollner A., Maier D., Albermann K., Hani J., Mokrejs M., Tetko I., Guldener U., Mannhaupt G., Munsterkotter M. and Mewes H.W. (2004) The FunCat, a functional annotation scheme for systematic classification of proteins from whole genomes. *Nucleic Acids Research* **32**: 5539-5545.

Sagi M., Omarov R.T. and Lips S.H. (1998) The Mo-hydroxylases xanthine dehydrogenase and aldehyde oxidase in ryegrass as affected by nitrogen and salinity. *Plant Science* **135**: 125-135.

Saito S., Hirai N., Matsumoto C., Ohigashi H., Ohta D., Sakata K. and Mizutani M. (2004) Arabidopsis *CYP707As* encode (+)-abscisic acid 8'-hydroxylase, a key enzyme in the oxidative catabolism of abscisic acid. *Plant Physiol*ogy **134**: 1439-1449.

Sakamoto A., Takeba G. and Tanaka K. (1990) Synthesis de novo of glutamine synthetase in the embryonic axis, closely related to the germination of lettuce seeds. *Plant and Cell Physiology* **31**: 677-682.

Schmidt A., Baumann N., Schwarzkopf A., Frommer W.B. and Desimone M. (2006) Comparative studies on Ureide Permeases in Arabidopsis thaliana and analysis of two alternative splice variants of *AtUPS5*. *Planta* **224**: 1329-1340.

Schubert K.R. (1986) Products of biological nitrogen fixation in higher plants: synthesis, transport, and metabolism. *Annual Review of Plant Physiology* **37**: 539-574.

Seki M., Ishida J., Narusaka M., Fujita M., Nanjo T., Umezawa T., Kamiya A., Nakajima M., Enju A., Sakurai T., Satou M., Akiyama K., Yamaguchi-Shinozaki K., Carninci P., Kawai J., Hayashizaki Y. and Shinozaki K. (2002) Monitoring the expression pattern of around 7,000 Arabidopsis genes under ABA treatments using a full-length cDNA microarray. *Functional and Integrative Genomics* **2**: 282-291.

Serventi F., Ramazzina I., Lamberto I., Puggioni V., Gatti R. and Percudani R. (2010) Chemical basis of nitrogen recovery through the ureide pathway: formation and hydrolysis of *S*-ureidoglycine in plants and bacteria. *ACS Chemical Biology* **5**: 203-214.

Sheoran I.S., Luthra Y.P., Kuhad M.S. and Singh R. (1981) Effect of water stress on some enzymes of nitrogen metabolism in Pigeonpea. *Phytochemistry* **20**: 2675-2677.

Shigeto J., Yoshihara S., Adam S. and Sueyoshi K. (2013) Genetic engineering of nitrite reductase gene improves uptake and assimilation of nitrogen dioxide by *Rhaphiolepis umbellata* (Thunb.) Makino. *Plant Biotechnology* **23**: 111-116.

Smith P.M. and Atkins C.A. (2002) Purine biosynthesis. Big in cell division, even bigger in nitrogen assimilation. *Plant Physiology* **128**: 793-802.

Stasolla C., Katahira R., Thorpe T.A. and Ashihara H. (2003) Purine and pyrimidine nucleotide metabolism in higher plants. *Journal of Plant Physiology* **160**: 1271-1295.

Todd C.D. and Polacco J.C. (2006) *AtAAH* encodes a protein with allantoate amidohydrolase activity from *Arabidopsis thaliana*. *Planta* **223**: 1108-1113.

Verslues P.E., Agarwal M., Katiyar-Agarwal S., Zhu J. and Zhu J.K. (2006) Methods and concepts in quantifying resistance to drought, salt and freezing, abiotic stresses that affect plant water status. *Plant Journal* **45**: 523-539.

Vogels G.D. and Van der Drift C. (1976) Degradation of purines and pyrimidines by microorganisms. *Bacteriol Reveiws* **40**: 403-468.

Wang P., Kong C.H., Sun B. and Xu X.H. (2012) Distribution and function of allantoin (5-ureidohydantoin) in rice grains. *Journal of Agricultual and Food Chemistry* **60**: 2793-2798.

Wasilewska A., Vlad F., Sirichandra C., Redko Y., Jammes F., Valon C., Frei dit Frey N. and Leung J. (2008) An update on abscisic acid signaling in plants and more. *Molecular Plant* **1**: 198-217.

Wasternack C. (1982) Metabolism of pyrimidines and purines. In: Pirson A. and Zimmermann M.H. (eds) *Encyclopedia of Plant Physiology*. New Series, Vol 14 B, Springer, Berlin pp 263-301.

Watanabe S., Nakagawa A., Izumi S., Shimada H. and Sakamoto A. (2010) RNA interference-mediated suppression of xanthine dehydrogenase reveals the role of purine metabolism in drought tolerance in Arabidopsis. *FEBS Letters* **584**: 1181-1186.

Werner A.K., Romeis T. and Witte C.-P. (2010) Ureide catabolism in *Arabidopsis thaliana* and *Escherichia coli*. *Nature Chemical Biology* **6**: 19-21.

Werner A.K., Sparkes I.A., Romeis T. and Witte C.-P. (2008) Identification, biochemical characterization, and subcellular localization of allantoate amidohydrolases from Arabidopsis and soybean. *Plant Physiol*ogy **146**: 418-430.

Werner A.K. and Witte C.-P. (2011) The biochemistry of nitrogen mobilization: purine ring catabolism. *Trends Plant Science* **16**: 381-387.

Xiong L., Lee H., Ishitani M. and Zhu J.K. (2002) Regulation of osmotic stress-responsive gene expression by the *LOS6/ABA1* locus in *Arabidopsis*. *Journal of Biological Chemistry* **277**: 8588-8596.

Xu Z.Y., Lee K.H., Dong T., Jeong J.C., Jin J.B., Kanno Y., Kim D.H., Kim S.Y., Seo M., Bressan R.A., Yun D.J. and Hwang I. (2012) A vacuolar ß-glucosidase homolog that possesses glucose-conjugated abscisic acid hydrolyzing activity plays an important role in osmotic stress responses in Arabidopsis. *Plant Cell* **24**: 2184-2199.

Yan J., Tsuichihara N., Etoh T. and Iwai S. (2007) Reactive oxygen species and nitric oxide are involved in ABA inhibition of stomatal opening. *Plant, Cell & Environment* **30**: 1320-1325.

Yang J. and Han K.H. (2004) Functional characterization of allantoinase genes from Arabidopsis and a nonureide-type legume black locust. *Plant Physiology* **134**: 1039-1049.

Yesbergenova Z., Yang G., Oron E., Soffer D., Fluhr R. and Sagi M. (2005) The plant Mo-hydroxylases aldehyde oxidase and xanthine dehydrogenase have distinct reactive oxygen species signatures and are induced by drought and abscisic acid. *Plant Journal* **42**: 862-876.

Zrenner R., Stitt M., Sonnewald U. and Boldt R. (2006) Pyrimidine and purine biosynthesis and degradation in plants. *Annual Review of Plant Biology* **57**: 805-836.